UNIVERSITY OF CENTRAL OKLAHOMA

Edmond, Oklahoma

Jackson College of Graduate Studies

**CHARACTERIZATION AND INCORPORATION OF MYCOBACTERIOPHAGE**

**FULBRIGHT INTO A POLYCAPROLACTONE NANOFIBER WOUND DRESSING**

A THESIS

SUBMITTED TO THE GRADUATE FACULTY

In partial fulfillment of the requirements

for the degree of

MASTER OF SCIENCE IN BIOLOGY

By:

Charmaine Moya Lopez-Davis

Edmond, Oklahoma

2022

CHARACTERIZATION AND INCORPORATION OF MYCOBACTERIOPHAGE FULBRIGHT INTO A POLYCAPROLACTONE NANOFIBER WOUND DRESSING

Thesis Title

## Charmaine Moya Lopez-Davis

Author's Name

## July 26, 2022

Date

Jackson College of Graduate Studies at the University of Central Oklahoma

A THESIS APPROVED FOR

THE DEPARTMENT OF BIOLOGY

By

Dr. Hari Kotturi

Digitally signed by Dr. Hari Kotturi
Date: 2022.07.26 14:52:26 -05'00'

Committee Chairperson

7/26/2022

Committee Member

Paul Olson

Digitally signed by Paul Olson
DN: cn=Paul Olson, o=Department of Biology,
ou=University of Central Oklahoma,
email=polson@uco.edu, c=US
Date: 2022.07.26 15:17:58 -05'00'

Committee Member

Committee Member

# ACKNOWLEDGEMENTS

**TABLE OF CONTENTS**

# LIST OF FIGURES

**Figure**                                                                                                                    **Page**

# LIST OF TABLES

**Table**                                                                                               **Page**

# GLOSSARY

**Acetone –** a colorless volatile liquid ketone made by oxidizing isopropanol, used as an organic solvent and synthetic reagent

**Acidemia –** an excessively acid condition of the body fluids or tissues

**Alkalemia –** a condition in which the hydrogen ion concentration in the blood is decreased

**Angiogenesis –** the development of new blood vessels

**Antibiotic resistance –** occurs when microorganisms such as bacteria and fungi develop the ability to defeat the drugs designed to kill them

**Antibiotics –** a medicine (such as penicillin or its derivatives) that inhibits the growth of or destroys microorganisms

**Antimicrobial Peptides –** inhibit cell division by inhibiting DNA replication and DNA damage responses, blocking the cell cycle, or causing the failure of chromosome separation

**Bacterial Cell Wall Hydrolase –** enzymes that degrade peptidoglycan (murein), a cross-linked heteropolymer that forms a mesh around the entire cell surface and confers mechanical strength and resistance against external turgor pressure

**Bacteriophage –** a virus that parasitizes a bacterium by infecting it and reproducing inside it

**Bacteriophage therapy –** uses viruses to treat bacterial infections

**Chemotactic –** orientation or movement of an organism or cell in relation to chemical agents

**Collagen –** the main structural protein found in skin and other connective tissues, widely used in purified form for cosmetic surgical treatments

**Complement factors –** system of plasma proteins that can be activated directly by pathogens or indirectly by pathogen-bound antibody, leading to a cascade of reactions that occurs on the surface of pathogens and generates active components with various effector functions

**Cytokines -** any of a number of substances, such as interferon, interleukin, and growth factors, which are secreted by certain cells of the immune system and have an effect on other cells

**Electrospinning –** a fiber production method that uses electric force to draw charged threads of polymer solutions or polymer melts up to fiber diameters in order of some hundred nanometers

**Endolysin –** enzymes used by bacteriophages at the end of their replication cycle to degrade the peptidoglycan of the bacterial host from within, resulting in cell lysis and release of progeny virions

**Fibroblast –** a cell in connective tissue which produces collagen and other fibers

**Growth factors –** a substance, such as a vitamin or hormone, which is required for the stimulation of growth in living cells

**Holin –** diverse group of small proteins produced by dsDNA bacteriophages in order to trigger and control the degradation of the host's cell wall at the end of the lytic cycle

**Hydophilicity –** having an affinity for water, readily absorbing or dissolving in water

**Hydrocolloid –** a substance which forms a gel in the presence of water, examples of which are used in surgical dressings and in various industrial applications

**Hydrogel –** a gel in which the liquid component is water

**Hydrophobicity –** repelling tending not to combine with, or incapable of dissolving in water

**Lysogen –** a bacterial cell or strain that has been infected with a temperate virus

**Lysozyme –** an enzyme that catalyzes the destruction of the cell walls of certain bacteria, occurring notably in tears and egg white

**Lytic phage –** the phage takes over the machinery of the bacterial cell to make phage components; they destroy and lyse the cell, releasing new phage particles

**Maxwell electrical stress** – represents the interaction between electromagnetic forces and mechanical momentum

**McFarland –** standards used in microbiology as a reference to adjust the turbidity of bacterial suspensions so that the number of bacteria will be within a given range to standardize microbial testing

**Microliter –** a unit of volume that represents one millionth of a liter

**Milliliter –** a unit of volume that represents one thousandth of a liter

**Multiplicity of Infection –** the ratio of agents (phages) to infection targets (bacterial cell)

**Mycobacteria –** a bacterium of a group which includes the causative agents of leprosy and tuberculosis

**Mycobacteriophage –** a member of a group of bacteriophages known to have the mycobacteria as host bacterial species

***Mycobacterium abscessus*** – a complex group of rapidly growing, multidrug-resistant, nontuberculous mycobacteria that are responsible for a wide spectrum of skin and soft tissue diseases, central nervous system infections, bacteremia, ocular, and other infections

***Mycobacterium smegmatis*** – an acid-fast, non-pathogenic species that has been used a s a model organism to study the genus *Mycobacterium*

**Neutrophils** – a type of white blood cell that is an important part of the immune system and helps the body fight infection; one of the first immune cells to respond when microorganisms enter the body

**Plaque** – a clearing of bacterial growth formed by infection of one bacterium by a single virus, which then progresses in a circular pattern

**Plaque forming unit** – a measure used in virology to describe the number of virus particles capable of forming plaques per unit volume

**Polycaprolactone** – a biodegradable polyester with a low melting point of around 60°C

**Polymer** – a substance that has a molecular structure consisting chiefly or entirely of a large number of similar units bonded together

**Proteinases** – enzymes that break down protein

**Purification** – removal of contaminants

**Sepsis** – a serious condition resulting from the presence of harmful microorganisms in the blood or other tissues and the body's response to their presence, potentially leading to the malfunctioning of various organs, shock, and death

**Superinfection immunity** - typically associated with lysogeny and appears to be a consequence of the same mechanisms that prevent prophage induction. Ecologically, superinfection immunity serves to prevent bacteria from being infected by two or more related prophage, or to protect the lysogen from being lysed.

**Taylor cone** – the cone observed in electrospinning, from which a jet of charged particles emanates above a threshold voltage

**Temperate phage** – a phage capable of replicating through the lysogenic cycle

**Tensile strength** – the resistance of a material to breaking under tension

**Titer** – the concentration of viruses expressed as infectious units per mL

**Virulence** – the severity or harmfulness of a disease or poison

# ABBREVIATIONS

**AMP –** antimicrobial peptides

**BC –** before Christ

**BCWH –** bacterial cell wall hydrolase

**CFU –** colony forming units

**DAMP –** damage associated molecular patterns

**DAPI –** 4′,6-diamidino-2-phenylindole

**DC** – direct current

**DNA** – deoxyribonucleic acid

**DSS –** diclofenac sodium salt

**EDC/NHS -** (N-ethyl-N′-(3-(dimethylamino)propyl)carbodiimide/N-hydroxysuccinimide)

**EO** – essential oils

**GFP –** green fluorescent protein

**HIV –** human immunodeficiency virus

**IFNγ** – interferon-γ

**IL-1β –** interleukin-1β

**IL-6 –** interleukin-6

**IL-10 –** interleukin-10

**IL-16 –** interleukin-16

**LPPO -** lypophosphonoxin

**MES –** 2-(N-morpholino) ethanesulfonic acid

**MOI –** multiplicity of infection

**NTM –** non-tuberculous mycobacteria

**OADC –** oleic albumin dextrose catalase

**PAMP –** pathogen associated molecular patterns

**PCL -** polycaprolactone

**PFU –** plaque forming units

**PLGA –** poly(lactic-co-glycolic acid)

**PPE –** personal protective equipment

**PU/EEP –** polyurethane/ethanolic extract of propolis

**RGM –** rapid-growing mycobacteria

**RHDV –** rabbit hemorrhagic disease virus

**RNA** – ribonucleic acid

**SGM –** slow-growing mycobacteria

**TNFα –** tumor necrosis factor-α

**VB-PAN/ZnO –** Viroblock-loaded polyacrylonitrile/zinc oxide

**VLPs –** virus like particles

**ABSTRACT OF THESIS**

**University of Central Oklahoma**

**Edmond, Oklahoma**

**NAME:** Charmaine Moya Lopez-Davis

**TITLE OF THESIS:** Characterization and incorporation of Mycobacteriophage Fulbright into a polycaprolactone nanofiber wound dressing

**DIRECTOR OF THESIS:** Hari Shankar R. Kotturi, Ph.D.

**PAGES: 88**

**ABSTRACT:** Nontuberculous mycobacteria infections such as *Mycobacterium abscessus* have become a growing concern due to the emergence of multidrug-resistant bacteria, making treatment of infections difficult. Bacteriophages, or phages, are viruses that can infect bacterial cells without harming eukaryotic cells. Bacteriophage therapy is a potential alternative for treating mycobacterial skin infections as phages only kill their bacterial host, leaving the normal flora unharmed.

Mycobacteriophage Fulbright was characterized and determined to possess qualities suitable for phage therapy. Fulbright remained stable at temperatures 20-60°C and pH 4-9. The replication cycle took approximately 3 hrs to complete, with a 90-minute latent phase. At high titer concentrations, Fulbright was able to lyse *M. abscessus*, a human pathogen. Fulbright was incorporated into polycaprolactone (PCL) fibers to serve as a model antibacterial wound dressing.

PCL_Fulbright effectively reduced the concentration of *M. smegmatis* and was observed to be non-toxic to fibroblast cells. Incorporated into the PCL fiber, the phage was stable for up to 11 months when stored at -20°C. This project is notable because it was the first mycobacteriophage incorporated into a nanofiber for phage therapy applications and serves as a foundation for future projects.

**CHAPTER 1: INTRODUCTION**

**1.1 Wound healing -** The skin is the largest organ in the human body and serves as the first line of defense against physical, chemical, and biological attacks (1, 2). The acidic nature of the skin and its sebum producing sebaceous glands make it difficult for pathogens to grow and infiltrate. When the skin is injured, there are four steps to wound healing: homeostasis, inflammation, tissue growth, and tissue remodeling (2).

A few minutes after an injury, platelets begin to stick to the wound site and to one another. Upon contact with collagen, platelets release the contents of their granules, and the production of thrombin converts fibrinogen to fibrin, initiating the coagulation cascade. This cascade activates fibrin to control the bleeding. Damage associated molecular patterns (DAMPs) and pathogen associated molecular patterns (PAMPs) are released at the site by dying cells and microorganisms, respectively. The DAMPs and PAMPs are picked up by pattern recognition receptors (PRRs) and trigger the activation of adaptive and innate immune responses. The neutrophils, macrophages, and keratinocytes are mobilized into the wound to phagocytize the pathogens present. Neutrophils secrete cytokines such as tumor necrosis factor-$\alpha$ (TNF$\alpha$), interleukin-1$\beta$ (IL-1$\beta$), and interluekin-16 (IL-16) to amplify the immune response. After the early innate response, adaptive immune responses act next via the antibody producing B-cells and cytokine secreting T-cells. Inflammatory cells and platelets release peptide growth factors that promote fibroblast migration to the wound site and activate angiogenesis. During this tissue growth phase, the fibroblasts form granulation tissue and deposition of extracellular matrix proteins like collagen. Angiogenesis helps in the development of new networks of blood vessels into the newly forming tissue to provide adequate oxygen and nutrients. Then, epithelialization occurs, where epithelial cells migrate from the wound

edges to the center. During the tissue remodeling stage, excess collagen fibers are degraded, and wound contractions begin to peak. Scar tissue is formed, and the wound is healed (2, 3, 4).

The healing process can take several weeks to months, depending on an individual's age, genetics, and lifestyle. Inadequate healing of wounds can lead to infection by microorganisms that can delay healing and worsen skin conditions (5). Throughout history, humans have always faced injuries and damage to the skin barrier. To combat this, wound dressings have been created and improved over the years.

**1.2 History of Wound Dressings** - A common way to promote wound healing is through the use of therapeutic wound dressings. Wound healing is a dynamic and complex process that requires a suitable environment to promote healing and return to homeostasis. A wound is a disruption in the continuity of epithelial lining of skin or mucosa that was caused by physical or thermal damage (6). There are two types of wounds: acute or chronic. Acute wounds are sudden but heal typically within 8-12 weeks, depending on the extent of damage (6, 7 ,8). Chronic wounds, however, do not progress through the normal stages of healing and do not normally resolve (6, 9). Local factors such as hypothermia and infections influence the characteristics of the wound, while systemic factors are the overall health or disease state of an individual that affects the ability to heal (6, 10). Of course, there are additional factors such as nutrition, age, and mineral deficiency that could prolong healing time (6).

Wounds need suitable dressing material to aid the healing process. The dressing quality should be based on its ability to: provide or maintain a moist environment; enhance epidermal migration; promote angiogenesis and connective tissue synthesis; allow gas exchange between tissue and environment; maintain temperature to improve blood flow to the wound and enhance

epidermal migration; provide protection against bacterial infection; non-adherent to the wound for easy removal or replacement; provide debridement action to enhance leucocyte migration and support enzyme accumulation; be sterile, non-toxic, and non-allergic (6).

Historically, both wet and dry dressings have been used for wounds. In 2500 BC, clay tablets were used for the treatment of wounds by Mesopotamians. In 1600 BC, linen was soaked in oil or grease and covered with plasters to occlude wounds. Wine or vinegar was used to clean the wounds that contained honey, oil, and wine, which was a practice followed by Hippocrates of Greece in 460-370 BC. During that time, they used wool boiled in water or wine as a bandage (6, 11). Antiseptic technique practices during the 19th century, as well as the introduction of antibiotics, allowed for proper control of infections and decreased mortality; however, the modern wound dressing that we know today was not available until the 20th century (6, 12).
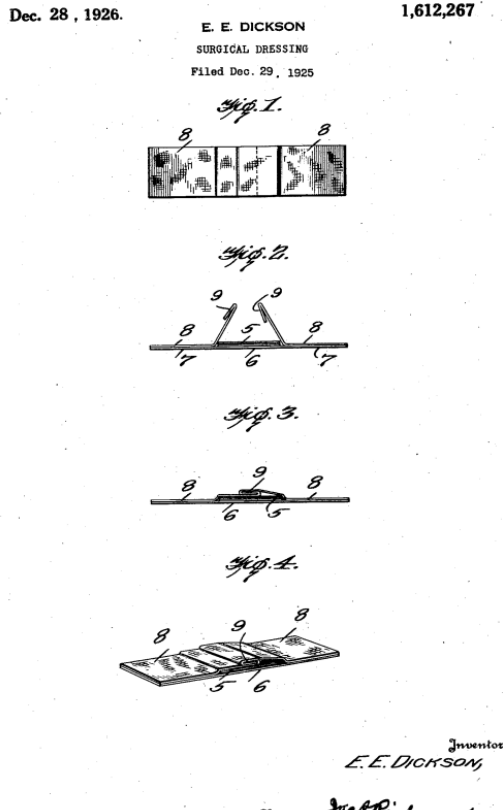
A dressing is ideal for enclosing the wound so that it is continuously exposed to proteinases, complement factors, growth factors, and chemotactic (6). In 1926, the first model of BAND-AID® was invented by Ensign Earle Dickson from New Jersey. This surgical dressing was to be used for cuts and other minor injuries. This dressing consisted of a gauze pad applied to the adhesive side of a band, with a covering that shields the pad and adhesive to maintain sterility (13). During the late 20th century,



Figure 1. First band-aid patent by E.E. Dickson.

3

the development of occlusive dressings began, which aided in faster re-epithelialization, collagen synthesis, promoted angiogenesis, and decreased wound pH to decrease risk of infection (6, 14). In the mid 1980's, the first modern wound dressings were introduced and had characteristics that provided moisture as well as absorbed fluids, and they contained materials such as hydrocolloids and iodine-containing gels. During the mid-1990's, synthetic wound dressings expanded into products that included hydrogels, hydrocolloids, alginates, synthetic foam dressing, silicone meshes, tissue adhesives, vapor-permeable adhesive films, and silver/collagen containing dressing.

Bioactive dressings are such as hydrogels and nanofibers are dressings that deliver substances active in wound healing and are typically derived from natural or artificial tissues, such as collagen, hyaluronic acid, chitosan, alginate, and elastin. Biological dressings, such as collagen dressings, are derived from a natural source and are sometimes incorporated with antimicrobials to enhance wound healing. (6, 15, 16, 17).

**1.3 Modern wound dressings** - Today, there are several types of dressings available for use. Semi-permeable film dressings are transparent and are composed of adherent polyurethane to permit oxygen and carbon dioxide transmission from the wound while impermeable to bacteria (6, 18). This allows the inspection of the wound and the healing process without the removal of the dressing; thus, these dressings were favorable for epithelializing wounds, superficial and shallow wounds. Examples are Opsite™, Tegaderm™, and Biooclusive™ (6).

Semipermeable foam dressings made up of hydrophobic and hydrophilic foam are also available, such as Lyofoam™, Allevyn™, and Tielle™. The hydrophobic properties of the outer layer protect from the liquid but allow gaseous exchange and water vapor. These types of dressings

are used for absorbing wound drainage from leg ulcers, exudating wounds, and granulating wounds. Semi-permeable foam dressings such as polyurethane foam are currently used to treat stage I-II burns and stage I-IV pressure ulcers; however, these dressings are not optimal due to the need for frequent replacement, and the effectiveness of these dressings depends on the severity of the exudative process (19). Hydrogel dressings, defined as highly hydrated polymer materials, meet most of the criteria for modern wound dressings due to high water content (70-90%), the ability to absorb wound exudate, maintain gas exchange, thermal insulation, presence of antibacterial properties, easier and less painful dressing changes, and reliable sterilization methods (6, 19, 20). In addition, the temperature of the wounds is decreased. Hydrogels are typically used for wounds that are dry, necrotic wounds, pressure ulcers, and burn wounds (6, 21). However, hydrogel wound dressings typically require a secondary dressing to ensure adhesion to the wound bed, such as a hydrocolloid, and require regular dressing changes of 2-3 days. Thus, hydrogel dressings should be non-adhesive or completely biodegradable (19). Some examples of hydrogel dressings are Intrasite[TM], Nu-gel[TM], Aquaform[TM], polymers, sheet dressings, impregnated gauze and water-based gels.

Hydrocolloid dressings are widely used, consisting of an inner colloidal layer and an outer water-impermeable later. These dressings are made up of carboxymethylcellulose, gelatin, and pectin combined with other materials (elastomers and adhesives). Though hydrocolloids are permeable to water vapor, they are impermeable to bacteria and have properties that absorb wound exudates (6, 20), typically used on pressure sores, minor burn wounds, and traumatic wounds. Some examples are Granuflex[TM], Comfeel[TM], and Tegasorb[TM]. Alginate dressings, made up of sodium and calcium salts, are absorbent and biodegradable. These dressings are made from seaweed. The absorption capability is due to the strong hydrophilic gel formation, limiting

bacterial contamination. However, some studies have reported that alginate inhibits keratinocyte migration, while other studies (22) reported that alginates accelerate the healing process by activating macrophages to produce TNF-a, which then initiates inflammatory signals (6).

Other dressings such as tissue-engineered skin substitutes that mimic the skin layer (Laserskin$^{TM}$, Biobrane$^{TM}$, Bioseed$^{TM}$, and Hyalograft3-DTM$^{TM}$. Drug-incorporated medicated dressings have also been used. Silver nanoparticle incorporated dressings are also available, which are made up of fibrous hydrocolloid, polyurethane foam film, and silicone gels. Antispetic iodine dressings are extremely effective against pathogens; however, iodine use can lead to skin irritation and staining. Composite dressings possess three layers and are versatile for use for both partial and full thickness wounds; however, they have less flexibility and are costly (6).

The diversity, as well as complexity of wound dressings available today are tailored to the type and severity of the wound; even so, no wound dressing is more advanced than the other in providing faster healing in chronic wounds. Because chronic wounds are typically associated with bacterial infections, it is imperative that wound dressing also provides an antibacterial component. Bacteriophages immobilized on polymer nanofibers is a promising antibacterial treatment towards wound infections (5).

**1.4 Bacteriophages** - Phages, or bacteriophages, are viruses that specifically infect bacteria. Bacteriophages can replicate using two pathways: the lytic and lysogenic pathway. Using its ligand, a phage can attach to a specific receptor found on the bacterial host surface and inject its genetic material into the host cell. The host provides enzymes and materials that are required for phage genome replication and production of progeny phage particles. The phage genome typically codes for proteins such as endolysin and holin which can lyse the host cell from within.

Holins accumulate in the host's cytoplasmic membrane and allow endolysin to degrade peptidoglycan, which allows the escape of progeny phage. Lytic phages take advantage of this mechanism through infection of neighboring cells, replication, and lysis. During a lysogenic cycle, temperate phage does not lyse the host immediately; instead, their genome is integrated into the host chromosome. When the phage DNA is integrated into a host genome, it is called a prophage, while the host bacterial cell is called a lysogen. The lysogenic cycle can be terminated due to stress or adverse environmental conditions which triggers the expression of phage DNA and the lytic cycle. Lytic phage have narrow host ranges; thus, using multiple phages is advantageous when performing phage therapy. Temperate phages in phage therapy have some disadvantages as well: phage genome can be inserted in the host chromosome, lay dormant, and even alter the phenotype of the host (23).

**1.5 Bacteriophage therapy** - Phage therapy, also called bacteriophage therapy, uses viruses to treat bacterial infections. Since these viruses can only attack bacteria, they are harmless to humans, plants, and animals. There are several commercial phage-based products with various targets such as food-borne bacterial pathogens on crops, animal feed, and food processing facilities. Animal models have demonstrated the efficacy in using phage therapy for bacterial infections (24), and human trials performed by Delmont Laboratories (USA) involving a product containing high concentrations of antistaphylococcal bacteriophages that were administered orally, intranasally, intravenously, and topically over 12 years only had minor side effects recorded (25). In 2020, a study conducted by the Alexander Tsulukidze National Centre of Urology in Tbilisi, Georgia consisted of a randomized, placebo-controlled, clinical trial on men 18 years of age and older, who were scheduled for transurethral resection of the prostate and had complicated urinary tract infection with no signs of systemic infection. The patients were given intravesical Pyo

bacteriophage, antibiotics, or a placebo. They found no significant difference between success rates in this study (26); however, phage titer, quality of administered phage preparations, and method of phage delivery play an important role in anti-bacterial activity of phages (27). In 2019, I.V. administration of an engineered phage cocktail, saved a 15-year-old patient from disseminated mycobacterial infection (28). For this project, the possibility of using bacteriophages to treat infected wounds was explored by incorporating the bacteriophage in nanofiber through a process called electrospinning.

**1.6 Electrospinning -** In 1887, Charles Boys introduced the idea of electrospinning when he reported that fibers could be produced from a viscous, elastic liquid and an external electrical field (29). Electrospinning uses electrostatic forces to generate synthetic fibers. A typical setup generates an electric field between the spinneret filled with polymer solution and a counter electrode at a distance by the drum collector. Though some researchers have shown minor success in using electrospinning methods for phage therapy applications, the success of the finished product is dependent on a variety of factors. First, the nanofibers should mimic the natural environment they will be used in, emphasizing the importance of choosing the type of polymer and materials for production (30). Besides the solvent and type of polymer, ambient conditions and processing parameters must be considered (31); for example, a high molecular weight polymer with a suitable solvent must be used for proper dissolution as low molecular weight polymers tend to produce beads instead of fibers. The evaporation rate and solidification rate of the jet is dependent on the volatility of the solvent. If the solvent is too volatile, the jet solidifies too quickly after exiting the spinneret; however, too low volatility produces wet fibers. Increasing the dielectric constant increases the voltage required to produce a stable jet. Since water has a high dielectric constant, it is not a favorable solvent for the dissolution of polymers through electrospinning (32),

which can be problematic as most phages are stored long-term in phage buffer, which consists mainly of water. A high concentration of polymer results in no jet formation, and low polymer concentration results in beaded droplets. A high viscosity leads to failed ejection of the solution from the spinneret, while a low viscosity produces very thin fibers. High electrical conductivity does not produce the Taylor cone, while perfectly insulated solutions cannot conduct charges (31). The flow rate, voltage, and distance between the collector and spinneret also affect the size and morphology of the fibers, as well as the temperature and humidity (33). Thus, all these factors must be considered and optimized when dealing with electrospinning nanofibers.

**1.7 Agents electrospun in PCL nanofiber** - Researchers from all over the world have demonstrated success incorporating various agents with polycaprolactone (PCL) through electrospinning. Cai and others (2014) proposed incorporating hyaluronic acid with PCL because hyaluronic acid maintains a moist wound environment and accelerates the in-growth of granulation tissue. They found that this bio-conjugated PCL membrane could bring on healing of a full-thickness wound compared to Mepitel, an antimicrobial wound contact layer product. tested on New Zealand white rabbits. Furthermore, the PCL membrane did not elicit a local or systemic inflammatory reaction and minimal scarring (34). In 2016, Carson and others loaded water-soluble anti-HIV drugs in various ratios of electrospun PCL and PLGA (poly-(lactic-co-glycolic) acid) and found that fiber compositions with higher PCL content yielded greater burst release, and fibers with higher PLGA content resulted in greater sustained release kinetics. They also found the drug-loaded fibers to be safe (cell viability remained at approximately 100% for all tested polymer concentrations) in vitro by exposing TZM-bL cells to various concentrations of fiber extract. (35).

Shin and others (2019) proposed a modified electrospinning method. Instead of randomly deposited nanofibers, they prepared radially patterned PCL fibers and observed mechanical and

biological properties compared to the traditional non-patterned PCL samples. They found no statistically significant difference in mechanical properties between the two types of PCL mates. However, their experiments indicated that migration occurs quicker in radially aligned nanofibers. This would mean that radially aligned PCL nanofibers could serve as potential material for biomedical applications, especially for tissue engineering or active tissue dressing material (36).

Siskova et al. (2021) investigated the in vitro biocompatibility of diclofenac sodium salt, a nonsteroidal, anti-inflammatory drug, (DSS)-loaded electrospun nanofiber mats on the base of PCL. They found a 92% viability of diploid human cell culture line composed of lung fibroblast (MRC 5) after 48 hours of incubation. They also tested the DSS-loaded fibers against CaSki and HeLa (cancer cells) and found significant activity (37).

Eskandarinia and others (2020) proposed that one-layer wound dressings are not sufficient in addressing all clinical needs and studied bilayer wound dressings, where they used a PCL/gel scaffold electrospun on a dense membrane composed of polyurethane and ethanolic extract of propolis (PU/EEP). The PU/EEP top layer was used to protect the wound from external contamination and dehydration, while the PCL/gel layer aided in cell adhesion and proliferation. They found significant antibacterial activity against *S. aureus, E. coli, and S. epidermidis* using inhibition zone test (38). Other researches such as Doostmohammadi et al. (2021) also explored the idea of PCL/gelatin fibers as potential wound dressings (39).

Oviedo and others (2021) developed two-bilayer membranes using chitosan and PCL and found that chitosan increased the hydrophilicity of the membranes, affecting the hemolytic behavior of the samples due to greater contact angle and anchoring points that favored the interrelation of the material with blood cells (40). Another group of researchers (41) also explored the incorporation of PCL/chitosan/Clay/curcumin and found that curcumin loaded films could

protect the wounds from bacterial infections. Safdari and others (2022) tested various natural antibacterial agents such as curcumin, piperine, eugenol, and rutin and electrospun them in PCL fibers, with three antibacterial agents loaded per fiber and found 74-75% antibacterial activity against Gram-positive bacterium and 96-99% antibacterial activity against Gram-negative bacterium (42).

Pham et al. (2021) demonstrated the antibacterial activity of lipophosphonoxin(LPPO)-loaded PCL fiber and the inability of the fiber to impair proliferation or differentiation of fibroblasts and keratinocytes in vitro. They also used a mouse model and observed that LPPO-loaded PCL significantly reduced *S. aureus* counts in infected wounds 7 days post-surgery while also promoting skin repair (43).

In 2022, Domingues and others explored the idea of antiviral face masks by incorporating various antiviral essential oils (EOs) in PCL through two methods: physisorption on pre-existing mats and blending the essential oils with the polymer solution prior to electrospinning. They found that lemongrass, Niaouli, and eucalyptus were the most effective EOs. Furthermore, they found that blending the EOs with the polymer prior to electrospinning were more mechanically and thermally resilient (44).

**1.8 Phage electrospun in PCL nanofiber** - In 2009, Liao and others encapsulated adenovirus encoding the green fluorescent protein (GFP) gene in PCL fiber cores through co-axial electrospinning and introduced an alternative mode of applying viral gene transfer. They found that when HEK 293 cells were seeded on these scaffolds, high levels of transgene expression were observed over a month, while cells inoculated by scaffold supernatant only showed transient expression for a week (45).

Nogueira et al. (2017) used polycaprolactone (PCL), a hydrophobic polyester that possess high elasticity and slow biodegradability (46, 47) as the polymer, which is advantageous because enzymes and microorganisms cannot breakdown PCL (48, 49). They observed a 99.9% reduction of *P. aeruginosa* upon contact with their phage fiber, and the bacteriophage vB_Pae_Kakheti25 remained stable after 20 minutes (5); however, an ideal wound dressing should be effective for longer than 20 minutes to prevent damage due to constant handling of the wound.

Choi et al. (2021) incorporated a T4 bacteriophage into polycaprolactone and tested its antimicrobial activity toward *Escherichia coli.* Choi tested two different methods of incorporating T4 into the fiber:  employing physical adsorption and chemical cross-linking. They found that chemically functionalized PCL film showed a larger lysis zone ($1.8cm^2$) than physically adsorbed film ($1.47 \text{ cm}^2$); in addition, chemically functionalized PCL was determined to produce a more homogenous distribution of phage T4 through fluorescence microscopy observations. Lastly, Choi tested the antimicrobial activity of chemically functionalized PCL with phage T4 as raw beef packaging material against *E. coli* and found that it was more efficient than the physically adsorbed fiber (50). Lee et al. (2004) incorporated aqueous suspensions of M13 bacteriophage into polyvinyl pyrrolidone, and the fibers demonstrated an instant release of the phage (51).

To explore the possibilities of using phage incorporated PCL for cutaneous infections, a high titer lysate of the bacteriophage must be obtained and incorporated into the polymer solution through electrospinning; in addition, the fiber should be imaged through scanning electron microscopy or transmission electron microscopy to validate the incorporation of the phage. Lastly, the phage fiber should be characterized by performing antimicrobial and cytotoxicity assays, as well as determining proper storage conditions.

# CHAPTER 2 - HYPOTHESIS AND OBJECTIVE

The objectives of this research are: 1) to characterize bacteriophage Fulbright by determining its stability at different pH and temperatures, testing its host range, and one-step growth curve; 2) to incorporate phage Fulbright into polycaprolactone (PCL) nanofiber and evaluating its efficacy in reducing *Mycobacterium smegmatis* concentration. Preliminary studies showed that Fulbright can also infect *M. abscessus* at high concentrations; therefore, demonstrating that Fulbright can be successfully incorporated in PCL without causing harm to normal cells can pave the way for phage therapy. My hypothesis is that electrospun nanofibers loaded with Fulbright phage will be effective in reducing *M. smegmatis* concentrations in vitro. The rationale for this proposed research is that although we have many ways to treat wound infections, no current treatment is truly effective without negative consequences. Heavy use of antibiotics has led to the emergence of multi-drug resistant bacteria. It can destroy the normal gut flora in the human body, causing an individual to be more susceptible to other infections. Silver nanoparticle dressings, bacterial cell wall hydrolases (BCWH), and antimicrobial peptides (AMPs) are alternatives to antibiotics but are costly or have documented negative consequences (5). Among all the different types of wound dressings available in the market, none have proved superior in treating chronic wounds, which are highly susceptible to bacterial infections. Successful incorporation of the phage Fulbright into PCL and an observed antimicrobial activity against the host *M. smegmatis* can contribute to phage therapy research.

To test the hypothesis, Fulbright was characterized by a) studying the phage stability in different temperature and pH conditions; b) performing one-step growth curve assay to undertand the life cycle of the virus with its host, *M. smegmatis.* The phage incorporated nanofiber (PCL_Fulbright) was also characterized by a) determining proper storage conditions; b) evaluating

PCL_Fulbright's efficacy against *M. smegmatis;* c) determining whether PCL_Fulbright can alter growth of a normal fibroblast mouse cell line.

# CHAPTER 3 – CHARACTERIZATION OF MYCOBACTERIOPHAGE FULBRIGHT ISOLATED FROM OKLAHOMA SOIL

**Title** – Characterization of Mycobacteriophage Fulbright isolated from Oklahoma soil

(This chapter represents work submitted to Proceedings of Oklahoma Academy of Sciences)

**Authors –** Charmaine Lopez-Davis[1], Cameron Kedy[1] & Ahmed K. Ali[2]

**Department affiliation -** [1]Department of Biology, University of Central Oklahoma, Edmond, OK 73034, USA

[2] Department of Biology, College of Science, Mustansiriyah University, Baghdad, Iraq

**Key Words: Mycobacteriophages, Fulbright, Phage one-step growth curve**

**Correspondence** – Hari Kotturi[1]

## Abstract

Cases of infections caused by non-tuberculous mycobacteria (NTM) have increased globally, affecting immune deficient children and adults. In fact, a 2009-2010 occurrence survey of NTP in potable water samples indicated an increased rate of *M. avium* (30%) and *M. abscessus* (12%). To determine if these findings correlate with human infections, clinical laboratory reports from four state health departments of the United States were used to investigate species of NTM isolated from human samples which increased from 8.2 per 100,000 persons in 1994 to 16 per 100,000 persons in 2014 (52). Furthermore, increasingly unsuccessful antibiotic remedies against emerging drug resistant bacteria makes research on alternatives to antibiotics paramount. In this project, we characterized the mycobacteriophage Fulbright, observed its ability to infect human pathogen *M. abscessus*, and explored the possibility of using it for phage therapy applications. We found that Fulbright is stable at pH 4-9 and temperatures 20-60°C. We observed a 90-minute latent period and a lytic burst plateau 3 h after adsorption. We observed that Fulbright can infect *M.*

*abscessus* at high concentrations ($1 \times 10^9$-$10^{11}$ PFU/mL). We electrospun Fulbright with polycaprolactone (PCL) nanofiber to serve as a model wound dressing and observed PCL_Fulbright successfully infecting *M. smegmatis.*

## 1. Introduction

The genus *Mycobacterium* is part of the order Actinomycetales and the phylum *Actinobacteria* and is composed of 170 species of bacteria that are aerobic, rod-shaped, and non-spore forming. They are lipid rich and acid-fast due to the long-chain mycolic acids in their cell walls; additionally, the mycolic acid makes it difficult to perform Gram staining, making this genus Gram-variable (53, 54). Mycobacterial species are ubiquitous due to multiple adaptations. For example, the lipid-rich hydrophobic outer membrane is a determinant of surface adherence, biofilm formation, aerosolization, and antibiotic/disinfectant resistance. Some species have evolved into potential human pathogens, presumably due to genomic events such as genome reduction, critical gene acquisition, gene transfer, mutations, and recombination (53, 55, 56, 57, 58).

Ubiquitous mycobacterial species are typically present in water and soil that humans encounter (53, 59, 60), and mycobacterial infections predominantly occur by entering through open skin and mucosal barriers, leading to cutaneous or pulmonary infections, respectively (61-64). Pathogenesis of cutaneous mycobacterial infections is the result of hematogenous dispersal, local or regional spread from a deep-seated infection, or a direct inoculation into the skin and soft tissues (53, 65). Modes of transmission of various mycobacterial species that cause cutaneous disease include zoonotic transmission (e.g. *M. bovis* foodborne transmission due to ingestion of

unpasteurized dairy products) (66, 67), person-to-person (e.g. *M. leprae*) (68, 69), vector-borne (*M. ulcerans*), and from environmental exposures (e.g. open skin injuries exposed to freshwater or salt water leading to infections caused by *M. marinum, M. ulcerans,* or *M. haemophilum)* (65, 70-75).

Nontuberculous Mycobacteria (NTM) are divided into two distinct groups: slow-growing mycobacteria (SGM) and rapid-growing mycobacteria (RGM) (76). *M. smegmatis* is a model organism that allows scientists to study the genus *Mycobacterium*. Using *M. smegmatis* is advantageous because it is not pathogenic and is an RGM (77, 78); additionally, it has been observed to be a part of the normal flora in human sebaceous gland secretions (79). The strain *M. smegmatis* mc$^2$155 is one of the most studied strains of *M. smegmatis* that was derived from the carbenicillin resistant parent strain, mc$^2$6 (80).

Nontuberculous Mycobacteria (NTM) cutaneous infections occur via direct inoculation through skin barrier damage from trauma, surgical procedures, tattoos, acupuncture, etc. (65, 81, 82), and there is some evidence of possible human-to-human transmission of *M. abscessus* subsp. *massiliense* in cystic fibrosis patients (83, 84). Infection with NTM is becoming a growing concern, surpassing the infection rate of tuberculosis in many industrialized countries (85, 86). Patients that suffer from NTM cutaneous infections typically possess other risk factors such as primary immunodeficiencies that are genetic or acquired (61, 63, 65, 87). In 1950, *Mycobacterium abscessus,* the most common cause of lung disease among the rapidly growing mycobacteria family, was first identified from a patient suffering from a knee infection. (88) Treatment of *M. abscessus* infections typically include antibiotics such as azithromycin and imipenem (89); however, a recent case of *M. abscessus* infection on a 15-year-old patient with cystic fibrosis

showed that the bacteria were not responsive to the antibiotic regimen given. The patient had also been on anti-NTM treatment 8 years prior to the lung transplantation that resulted in chronic infections. The patient was discharged 7 months post-transplant with a diagnosis of disseminated mycobacterial infection that began in the lungs and spread to the arms, legs, and buttocks. Researchers genetically engineered a cocktail of phages that were collected by students in the Science Education Alliance Phage Hunters Advancing Genomics and Evolutionary Science (SEA-PHAGES) program that were observed to infect *M. abscessus* in vitro. Intravenous administration of the cocktail was given over several months and the patient continued to improve with gradual healing of surgical site and skin lesions. Patient sera did not show evidence of phage neutralization and weak cytokine responses (IFNγ, IL-6, IL-10, TNF α) were observed (28).

As bacteria continues to develop resistance to current accepted treatments such as antibiotics, there is a growing need for alternative methods of treatments. Bacteriophage therapy presents as a promising alternative due to their narrow host range. However, the very nature of bacteriophages is still poorly understood. There are more than $10^{31}$ phage particles in the biosphere, and if the phages were laid end to end, they would extend from Earth to the Sun $10^{13}$ times (90). Viral ecologists calculate that there are about $10^{23}$ phage infections per second on a global scale, which indicates that this population is large, ancient, and highly dynamic (91, 92).

Despite bacteriophages being present for billions of years, there are no records of their origins; thus, the best way to understand phages and their evolution is through analysis of phages in the environment today. A prominent feature of bacteriophages is their pervasively mosaic genome, with different segments having apparent evolutionary histories (92, 93). The viral genome, which is composed of either DNA or RNA, is encapsulated by the viral capsid made up

of capsomeres that are linked via peptide, disulfide, and hydrogen bonding, as well as van der Waals interactions (79, 94-97). The nucleocapsid consists of both the genomic material and the capsid shell. Enveloped viruses, which mainly infect animal cells, obtain the envelope layer from the host's plasma membrane, endoplasmic reticulum, or Golgi body. Enveloped viruses escape their host cell through budding, a process where the virus leaves the infected cell without killing it. However, non-enveloped viruses, or naked viruses, leave their host through lysis, a common strategy utilized by bacteriophages (97, 98).

Mycobacteriophages are phages (viruses) that specifically infect mycobacteria. Following the discovery of bacteriophages, interest in mycobacteriophages arose in the late 1940s when they were first isolated (99, 100). After successful isolation, mycobacteriophages were first utilized for the typing of clinical *Mycobacterium* spp. due to the narrow host range of phages (100, 101). As technological advances have made new sequencing technologies possible, there are at least 2125 mycobacteriophage genomes isolated and sequenced (102). Because mycobacteriophages can act as bactericidal agents, they could be used directly to destroy bacterial hosts, or phage-encoded products such as lysins could be used against pathogens (103). Since phages can also inhibit the metabolism of their hosts (host inactivation) (103, 104), deeper mechanistic understanding could lead to another potential strategy. Thus, studying mycobacteriophages and characterizing them could help find alternative treatments for mycobacterial pathogens. In this study, we characterized a previously isolated and sequenced mycobacteriophage Fulbright by 1) testing phage stability in various pH conditions; 2) testing phage stability in temperature conditions; 3) observing phage-host interaction using a one-step growth curve assay; 4) testing the efficacy of Fulbright in killing *M. abscessus*. Lastly, we incorporated phage Fulbright into polycaprolactone (PCL_Fulbright) to

serve as a potential antibacterial wound dressing and tested its efficacy against *M. smegmatis* and *M. abscessus* bacterial lawns.

## 2.  Materials and Methods

*2.1 Culture medium and bacterial culture preparation*

*Mycobacterium smegmatis* mc$^2$155 provided by the Hatfull lab at the University of Pittsburgh (Pittsburgh, PA, USA) was grown in the standard 7H9 liquid medium complete (7H9 broth base, 0.2% glycerol, albumin dextrose catalase (ADC) (10%V/V), 1 mM calcium chloride (CaCl$_2$)) and incubated in a shaking incubator (Fisher Scientific # SHKE4450). On solid media, the bacteria were grown on the standard 7H10 agar plates (0.5% glycerol, 0.2% dextrose, and 1 mM calcium chloride (CaCl$_2$)). Cultures grown were incubated at 37 °C. 50 µg/mL of cycloheximide and 50 µg/mL of carbenicillin were added to the liquid culture medium and 7H10 agar plates to reduce contamination. 2X Middlebrook top agar (7H9 broth base, 0.8% agar) was diluted at a 1:1 ratio with 7H9 liquid medium neat (7H9 broth base, 0.2% glycerol, 1 mM calcium chloride (CaCl$_2$) to make 1X Middlebrook top agar, which was used to plate the bacterial lawn. The phage lysate was diluted in phage buffer (pH 7.2, 10 mM Tris, 10 mM magnesium sulfate (MgSO$_4$), 70 mM sodium chloride (NaCl), and 1 mM CaCl$_2$ to quantify the phage. For the agar-overlay method, 10 µL of each dilution was added to 250 µL of *M. smegmatis* mc$^2$155 bacteria and incubated for 10 min. After incubation, 4.5 mL of 1X Middlebrook top agar was added to the bacteria and phage mixture and transferred to a 7H10 agar plate. The plates were incubated at 37 °C and assessed for plaques. *Mycobacterium abscessus* ATCC 19977 were grown in similar conditions as *M. smegmatis* without cycloheximide and carbenicillin addition. Middlebrook 7H10 Oleic Albumin Dextrose Catalase (OADC) supplementation (cat #MBS652952) was used instead of calcium chloride, dextrose, and glycerol to improve bacterial growth.

*2.2 Phage Fulbright stability in pH conditions*

The stability of the mycobacteriophage was evaluated by incubating the phage in phage buffer adjusted to pH values (2, 3, 4, 5, 6, 7, 8, 9, 10, 11, 12) at room temperature for 1 h following the protocol described in previous publications (105, 106). The pH of the phage buffer was adjusted using HCl or NaOH and was 0.22 μm filter-sterilized. The initial concentration of phage was $1 \times 10^{11}$ PFU/mL, and it was incubated for 1 h at room temperature. Following the 1 h incubation, the phage solution was diluted, plated using the agar-overlay method, and incubated at 37 °C prior to assessment of plaques.

*2.3 Phage Fulbright stability in thermal conditions*

The stability of phage Fulbright was evaluated at different temperatures (20°C, 30°C, 40°C, 50°C, 60°C, 70°C, 80°C), following the protocol described in previous works (105, 106). 1 mL volume of the phage lysate ($1 \times 10^{11}$ PFU/mL) was dispensed onto a 1.5 mL tube and incubated at the temperature conditions for 1 h. Following thermal incubation, the lysates were serially diluted in sterile phage buffer and then plated using the standard agar-overlay method. After incubation, the number of PFU/mL was determined and plotted. The PFU/mL was measured at 60 minutes of incubation.

*2.4 One-step growth curve of Fulbright*

The one step growth curve was done at a multiplicity of infection (MOI) of 1.0 (one bacterial cell to one bacteriophage) following protocol from previous work with mycobacteriophages (106). The host bacterium and phage were incubated at 37ºC for 50 minutes to allow for complete phage adsorption. Following incubation, 0.4% sulfuric acid ($H_2SO_4$) was added to inactivate unattached phage particles, and the solution was incubated again for 5 minutes at room temperature. The $H_2SO_4$ was neutralized by adding 0.4% sodium hydroxide (NaOH). The

bacteriophage suspension was diluted in 7H9 broth and incubated at 37 ºC. Every 30 minutes, for a duration of 8 hours, the sample solution was diluted and plated using the double agar layer method. Following incubation, the plaques were counted to determine PFU/mL and plotted.

*2.5 Comparing the efficacy of Fulbright against <u>M. smegmatis</u> and <u>M. abscessus</u>*

Bacterial lawns were plated on standard 7H10 agar plates by mixing 250 uL of bacteria with 4.5 mL of standard 7H9 Middlebrook 1X top agar. *M. abscessus* ATCC 19977 was plated on standard 7H10 agar supplemented with OADC, while *M. smegmatis* mc$^2$155 was supplemented with 0.5% glycerol, 0.2% dextrose, and 1 mM calcium chloride (CaCl$_2$). 5 uL of serially diluted Fulbright lysate was spotted onto bacterial lawn. Plates were incubated right side up overnight to allow spots to absorb and were flipped upside-down the next day. *M. smegmatis* plates were incubated for 2 days, while *M. abscessus* plates were incubated up to 6 days.

*2.6 Comparing effectivity of PCL_Fulbright against host bacteria M. smegmatis and M. abscessus*

Phage Fulbright was incorporated into polycaprolactone (PCL) fiber using methods described in our previous work (105). After electrospinning, ~2cm$^2$ of the phage incorporated fiber was cut and plated on agar plates containing host bacterial lawn, *M. smegmatis* or *M. abscessus.* The plates were incubated at 37°C for 48 hours and assessed for clear borders surrounding the fiber.

*2.7 Data analysis*

All experiments were performed in triplicates unless otherwise noted. GraphPad prism was used to calculate one-way ANOVA and Tukey post hoc tests and establish multiple comparisons between samples. A p-value below 0.05 were considered statistically significant.

## 3. Results and Discussion

There has been a growing interest in studying mycobacteriophages as possible bactericidal agents due to the growing problem of highly pathogenic mycobacterial species such as *M. tuberculosis and M. abscessus.* To determine suitable phages for phage therapy applications, isolation, identification, and full characterization of the phage, while using reliable and reproducible methods, is necessary (107). Here, we characterized previously isolated mycobacteriophage Fulbright by testing its stability at different temperature and pH conditions. Certain conditions such as extreme temperatures can denature the protein capsid shell of phages, and extreme acidic or alkaline conditions can react chemically with proteins or nucleic acids to inactivate phages (108). Temperature has also been found to affect the phage replication mechanism. For example, experiments on a phage infecting the host *B. thailandensis* showed that at higher temperatures (37°C), the phage undergoes a lytic cycle, but remains temperate at lower temperatures (25°C) (109). In fact, various studies have emphasized the importance of temperature on host-phage interactions (110-115). Extreme pH values cause hydrogen ions and hydroxyl ions to be highly concentrated in the water, resulting in viral inactivation (108). Because highly reactive radicals in a water environment (such as hydroxyl and superoxyl ions) have a long lifespan, they oxidize materials in the environment and can affect phage capsid shell by removal, deformation, or denaturation of critical ligand sites and overall dissociation of the capsid. Once the protein shell has been degraded, RNA hydrolysis could occur inside or outside the phage particle, resulting in the loss of infectivity (108)

Our results showed that mycobacteriophage Fulbright is stable for up to 60 minutes when exposed to temperatures 20-60°C, and the phage particle is inactivated at 70°C and above (Figure

2). In contrast, other novel mycobacteriophages described in Stella et al. (2013) were isolated at 30°C and were unable to propagate at a higher temperature of 37°C. Phage Cepens was found to be unstable at temperatures 37°C and higher (116). Our results are comparable to bacteriophages against *Vibrio parahaemolyticus*, which retained infectivity between 25-50°C (117).

pH stability assays showed that Fulbright is stable in pH 4-9, with a ten-fold decrease at pH 3. There was a significant difference in phage titer between pH 3 and 4 ($p<0.0001$). No viable plaques were observed at pH 2, 10, 11, and 12 (Figure 3). Various phages that infect other hosts such as *E. coli, Pseudomonas,* and *Vibrio* have been characterized and observed to behave similarly, with significant reduced viability at a pH of 3 and below (107, 118, 119). *Vibrio* phages studied by Yin and others (2019) were found to retain activity at a broad range of pH 2-12 (120). In contrast, mycobacteriophage Cepens showed stability in a narrow pH range of 7-9 (116).

Because Fulbright can maintain stability in a wide range of temperature and pH conditions, it serves as an excellent candidate for phage therapy. The human body at homeostasis is 37°C, and upon infection and/or sepsis, the body temperature typically climbs to 38°C and higher. Thus, Fulbright can endure these higher temperatures if used for therapy. The human saliva has a typical pH range of 6.2-7.6 (121). The human blood has a normal pH range of 7.35-7.45 (122), and values greater than 7.8 (alkalemia) or less than 6.8 (acidemia) often result in death. Lastly, open wounds are characterized to have a neutral to alkaline pH of around 6.5 to 8.5, while chronic wounds exist at a range of 7.2 to 8.932 (123). Fulbright is stable from pH 4-9 and can thus be used for oral, intravenous and cutaneous applications. Ingestion of the phage would not be favorable as Fulbright begins to destabilize at a pH of 3 and lower which are optimal pH conditions for human stomach (124).
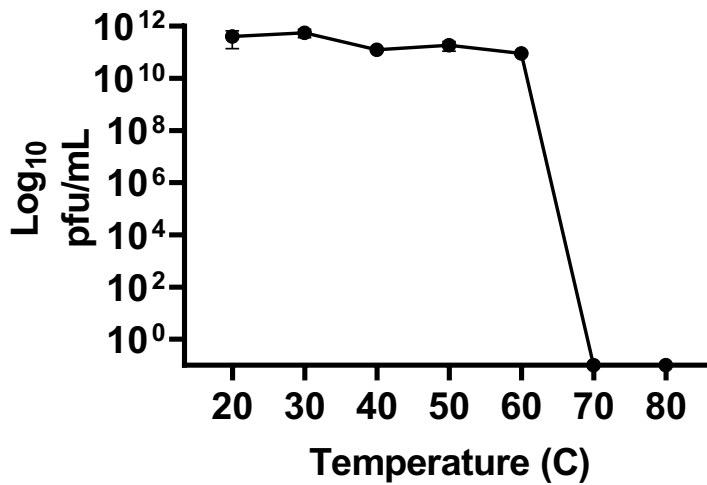
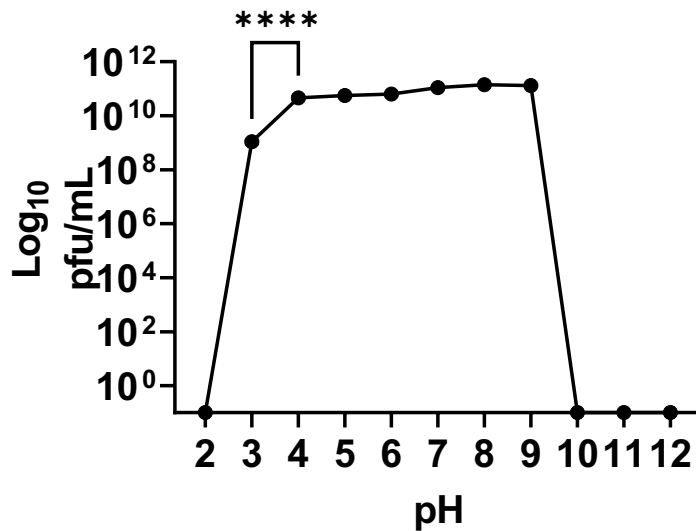Figure 2. Temperature stability of phage Fulbright



Figure 3. pH stability of phage Fulbright. ****p<0.0001

Because a good understanding of a phage's latent period is needed to determine its potential use for phage therapy, we constructed a one-step growth curve for phage Fulbright. We found the latent period of phage Fulbright to be 90 min, followed by a rise period of 90 min. The PFUs plateaued after the rise period, approximately 3 h after adsorption (Figure 4). These results are similar to previous work with mycobacteriophages (106). Kalapala et al. (2020) tested the infectivity of mycobacteriophages at various multiplicity of infection (MOIs) (10, 1, 0.1, and 0.01),

and found that MOI of 10 and 1 both significantly reduced bacterial growth 3 h post treatment

(125). Bavda and Jain (2020) observed a latent period of 60 minutes for mycobacteriophage D29;

moreover, when they generated a D29 holin knockout phage, the latent period increased to 90

minutes (126). Studies by Fan et al. (2016) showed mycobacteriophage SWU1 to have a latent

period of 30 minutes and a burst time of 270 minutes (127). BO1 and BO2a phages had latent

periods of 150 min and 260 min, respectively (128). Samaddar used a different approach to observe

mycobacteriophage-mycobacterial host interaction and used flow cytometry to measure bacterial

cell viability. Samaddar also found similar results with a ~60 min latent period (129).
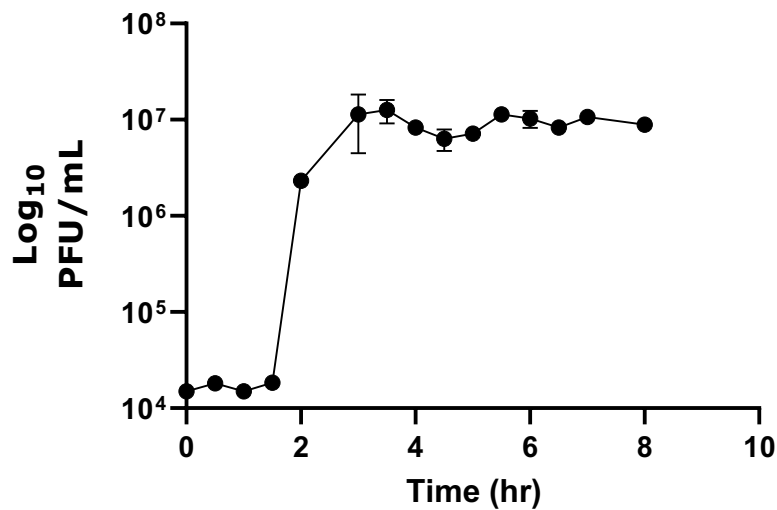


Figure 4. One-step growth curve of phage Fulbright.

To determine whether Fulbright is a good candidate for phage therapy applications for

treating human mycobacterial infections, we also tested the efficacy of Fulbright against human

pathogen *M. abscessus.* Results showed that at high concentrations, Fulbright can effectively lyse

*M. abscessus.* Figure 5b shows Fulbright is effective up to $10^{-2}$ dilution in lysing the host cell.

These results are comparable to preliminary work done with Fulbright (130). This limited

infectivity against *M. abscessus* has also been observed by the Hatfull lab, where phages (Muddy,

ZoeJ, and BPs) were first isolated using host *M. smegmatis*. The three phages were genetically modified and engineered to improve infectivity against *M. abscessus* subsp. *massiliense* and were then intravenously administered to the previously described cystic fibrosis patient, making it the first therapeutic use of phages for a human mycobacterial infection. (28). Phage Fulbright has the potential for therapeutic use in a similar fashion.
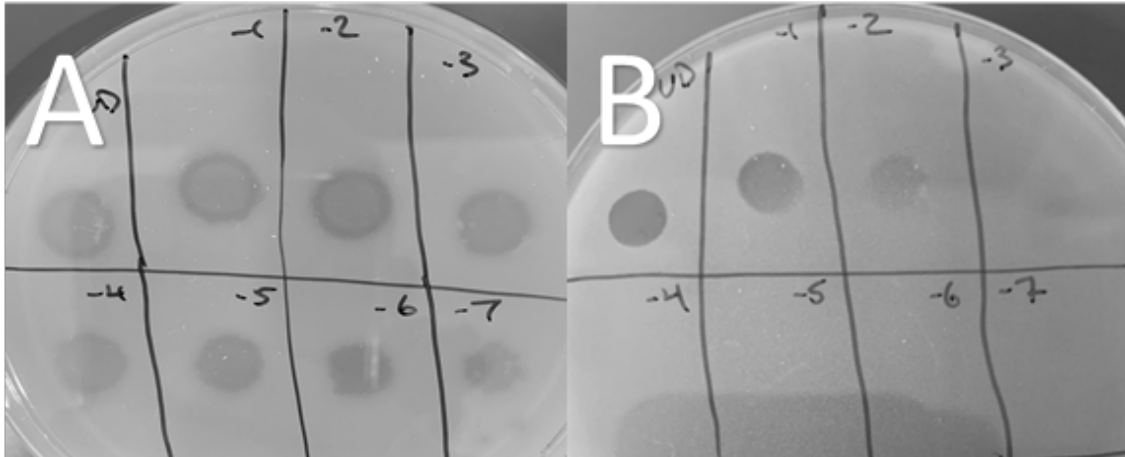


Figure 5. Testing host range of phage Fulbright. Fig 5a shows spot test results at ten-fold dilutions against *M. smegmatis*; Fig 5b shows that Fulbright can lyse *M. abscessus* at high titer.
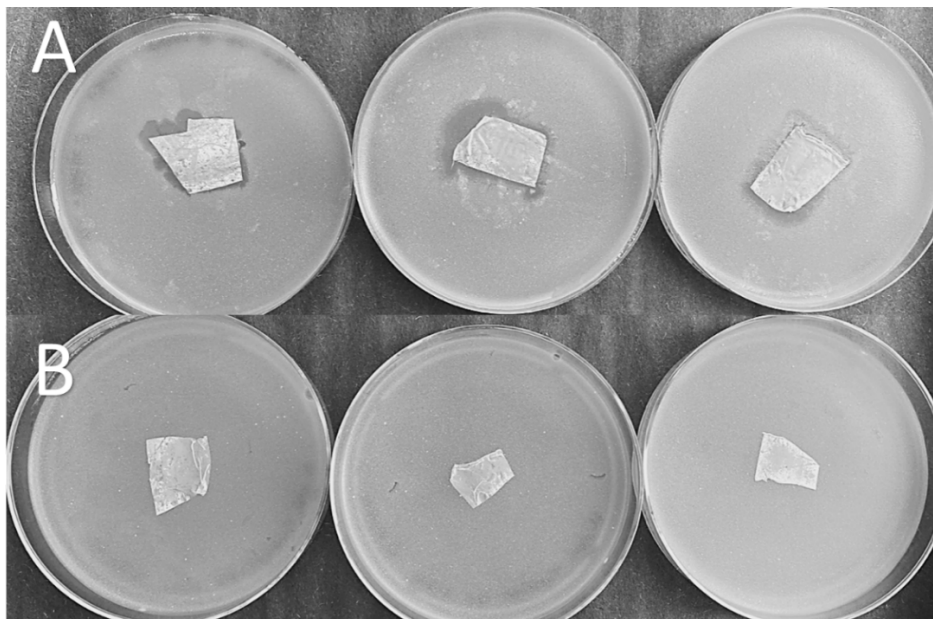


Figure 6. Testing the effectivity of phage Fulbright incorporated PCL against *M. smegmatis* bacterial lawn (Fig 6a) and against *M. abscessus* (Fig 6b). Clear lysis zones surrounding the edges of the fiber on Figure 5a shows that the fiber is effective in killing *M. smegmatis,* but not *M. abscessus* (Fig 6b).

In our previously published work with Fulbright (105) we successfully incorporated our phage into a PCL wound dressing. We tested phage incorporated fiber against against *M. smegmatis* and *M. abscessus*. Our results showed PCL_Fulbright to be effective against *M. smegmatis* (Figure 6a)*,* but not *M. abscessus* (Figure 6b)*.* A possible reason for this is the low-concentration and slow release of phage Fulbright from the nanofiber. We previously observed that ~2cm$^2$ of PCL_Fulbright released +/−2.1 × 10$^5$ PFU/mL infectious particles after 1 h incubation in 1 mL of phage buffer. Another reason that PCL_Fulbright was able to infect *M. smegmatis* but not *M. abscessus* could be due to the properties of mycolic acid present. Mycolic acids are a major component of mycobacterial cell walls (131-134), and despite providing similar functions in all mycobacterial pathogens (cell protection, virulence, structural integrity), subtle differences in the carbon chain length are found that may contribute to their susceptibility to infections (131). Furthermore, we hope to optimize the effectivity of the phage fiber by improving our electrospinning techniques via increasing porosity and hydrophilicity, or by incorporating other materials such as collagen and hydrogel in order to increase the phage release and infectivity while promoting optimal conditions for appropriate wound healing.

Bacteriophages have the potential for therapeutic and food safety uses due to their ability to lyse multi-drug resistant pathogens (107). They are low cost, easy to manufacture, and have no documented side effects to date. Our research lays a good foundation for continuing research and possible application of Fulbright in the future.

**Acknowledgements**

# CHAPTER 4 - INCORPORATION OF MYCOBACTERIOPHAGE FULBRIGHT INTO POLYCAPROLACTONE ELECTROSPUN NANOFIBER WOUND DRESSING

**Title -** Incorporation of Mycobacteriophage Fulbright into Polycaprolactone Electrospun Nanofiber Wound Dressing

**Authors -** Hari Kotturi[1], Charmaine Lopez-Davis[1], Sadegh, Nikfarjam[1], Cameron Kedy[1], Micah Byrne[1], Vishal Barot[2], and Morshed Khandaker[2]

**Department affiliation –** [1]Department of Biology, University of Central Oklahoma, Edmond, OK 73034, USA

[2]Department of Engineering and Physics, University of Central Oklahoma, Edmond, OK 73034, USA

**Correspondence –** Hari Kotturi, Charmaine Lopez-Davis, and Morshed Khandaker

**Abstract -** The genus *Mycobacterium* includes pathogens known to cause disease in mammals like tuberculosis (*Mycobacterium tuberculosis*) and skin infections (*M. abscessus*). *M. smegmatis* is a model bacterium that can cause opportunistic infections in human tissues and, rarely, a respiratory disease. Due to the emergence of multi-drug resistant bacteria, phage therapy is potentially an alternative way of treating these bacterial infections. As bacteriophages are specific to their bacterial host, it ensures that the normal flora is unharmed. Fulbright is a mycobacteriophage that infects the host bacteria *M. smegmatis*. The main goal of this study is to incorporate Mycobacteriophage Fulbright into a polycaprolactone (PCL) nanofiber and test its

antimicrobial effect against the host bacteria, *M. smegmatis*. Stability tests conducted over 7 days showed that phage titer does not decrease when in contact with PCL, making it a promising vehicle for phage delivery. Antimicrobial assays showed that PCL_Fulbright effectively reduces bacterial concentration after 24 hours of contact. In addition, when stored at -20ºC, the phage remains viable for up to eleven-months in the fiber. Fulbright addition on the nanofibrous mats resulted in an increase in water uptake and decrease in the mechanical properties (strength and Young's modulus) of the membranes, indicating that the presence of phage Fulbright can greatly enhance the physical and mechanical properties of the PCL. Cytotoxicity assays showed that PCL_Fulbright is not cytotoxic to Balbc/3T3 mouse embryo fibroblast cell lines; thus, phage-incorporated PCL is a promising alternative to antibiotics in treating skin infections.

**1. Introduction -** Bacteriophage therapy, which uses bacterial viruses (phages) to treat bacterial infections, has been around for almost a century. During 1915, an outbreak of severe hemorrhagic dysentery among French troops in Paris occurred, and Felix d'Herelle was assigned to investigate the outbreak. He made bacterium-free filtrates of the soldiers' fecal samples and incubated them with Shigella strains isolated from patients. A portion of the mixture was spread on an agar medium to observe bacterial growth, and he observed the appearance of clear plaques. He presented his findings during the Academy of Sciences meeting in 1917. Soon after discovering bacteriophages, d'Herelle used phages to treat Shigella dysenteriae in 1919, which was most likely the first attempt to use bacteriophages therapeutically (135). However, the very existence of phages was not truly confirmed until the invention of electron microscopy in the 1940s (136, 137).

Unreliable experimental success and poor documentation of studies led to reduced efforts for further phage research; moreover, the biological nature of phages was poorly understood.

Rudimentary technical practices and improper storage resulted in low phage titers and contamination. In addition, medical limitations during that time made it unfeasible to find methods of phage delivery to infection sites (136). While Western medicine dismissed phage therapy, the former Soviet Union and Eastern Europe continued to study phage therapy and conducted trials to treat a range of infectious agents such as Staphylococcus, Pseudomonas, and E. coli (138, 139).

During the 1900s, major causes of death were infectious diseases such as cholera, diphtheria, syphilis, and many others. By the mid-20th century, the use of antibiotics and better sanitation practices prolonged life expectancy and improved the quality of life. However, it did not take long for bacteria to adapt and evolve, and they became equipped with antibiotic resistance genes such as ß-lactams, aminoglycosides, chloramphenicols, and tetracycline (136). Antibiotic resistance genes are dangerous especially for difficult-to-treat infections such as Mycobacterium abscessus, which is a nontuberculosis mycobacteria that can cause disease to the skin, soft tissue, and central nervous system (140, 141). In the United States alone, around 2.8 million multidrug-resistant infections occur annually resulting in over 35,000 deaths (142). Skin and soft tissue infections (SSTIs) are common types of infections that affect approximately 14 million people annually in the United States (143-145). It is imperative that alternative treatments to bacterial infections are studied to preserve the length and quality of human life.

Thus, recent studies have focused on three groups of antimicrobials as alternatives to antibiotics: bacterial cell wall hydrolase (BCWH), antimicrobial peptides (AMPs), and bacteriophage (146). BCWH has some disadvantages because it cannot be used toward Gram-negative bacteria due to the outer membrane, and some Gram-positive pathogens are already resistant to lysozymes. AMPs are effective against a plethora of bacteria and fungi but are costly and require high, toxic doses. Bacteriophage are promising, since they are highly specific, can

infect both Gram-positive and Gram-negative bacteria, and are low-cost (5). The specificity of bacteriophage to their bacterial host also ensures that normal microorganisms that are already present on the skin and are beneficial to the body remain unharmed.

Bacteriophage therapy can be performed in a plethora of ways. Topical applications have shown success when a study conducted by the Wound Centers at St. Joseph's Medical Center in Tacoma used Staphylococcus aureus phages to treat diabetic toe ulcers of nine patients. The phage solution was applied to the ulcers once a week, and all infections responded to the phage therapy, and the ulcers healed within approximately seven weeks (147). However, liquid and semi-solid gel formulations may be expensive and inconvenient to transport and store. The United States Army investigated the use of bacteriophages for food and safety and determined that phages must be stored and shipped dry to reduce the size and weight. While drying methods such as lyophilization or freeze drying is feasible, this can be expensive and time consuming. Thus, a promising method of phage application on skin infections is through electrospinning (148).

Electrospinning is a common method used to produce nanofibers with a diameter in the range of 100 nm or less (149). A polymer solution is supplied from a spinneret, and a droplet forms at the spinneret exit. An electrical field is applied to the solution by placing an electrode in it and a counter-electrode at a distance from the spinneret. The Maxwell electrical stress stretches the droplet, and a Taylor cone forms due to the repulsion of the molecular charges, resulting in the ejection of a charged jet (149, 150). The ejected jet extends in a straight line and undergoes vigorous whipping due to bending instabilities. The jet continues to stretch and dry as the solvent eventually evaporates, and the spun nanofibers are deposited on the counter electrode (149).

There are several studies that have shown success with materials incorporated in electrospun fiber. A study by Salam et al. (2021) designed an electrospun nanofiber-based

Viroblock (VB)-loaded polyacrylonitrile (PAN)/zinc oxide (ZnO) hybrid nanocomposite for personal protective equipment (PPE) applications. Their results showed an antibacterial activity of 92.59% and 88.64% against Staphylococcus aureus and Pseudomonas aeruginosa, respectively (151). Dowlath et al. (2021) electrospun rabbit hemorrhagic disease virus (RHDV) Virus Like Particles (VLPs) as an antigen carrier into a polyvinylpy-roolidone (PVP)-based nanofiber and successfully showed that all treatments that contained the VLP induced an antibody response (152). A study conducted by Kazsoki et al. (2022) showed the potential of using formulated core–shell-type nanofibrous scaffolds loaded with dexpanthenol (shell) and acyclovir (core) as an alternative treatment of herpes labialis (153).

Polycaprolactone (PCL) has been widely used in a large range of biomedical applications such as wound healing, drug delivery, and bone regeneration (153-158). PCL is a hydrophobic polyester that has high elasticity and slow biodegradability; moreover, PCL cannot be easily broken down by enzymes and microorganisms, making it a promising method of phage delivery (5). PCL is an aliphatic polyester belonging to the poly-α-hydroxy group (159) and is mainly degraded through hydrolysis of ester bonds on its molecular chains, generating carboxylic acid and hydroxyl functional groups, which reduces the molecular weight and decreases the overall weight of the polymer. The biodegradation rate of PCL is affected by its molecular weight, molecular weight distribution, crystallinity, and hydrophobicity of PCL molecular chains (156, 160). Many studies have shown great success incorporating various materials with PCL and demonstrated antimicrobial properties. He et al. (2021) constructed a sandwich-like dressing approach, with the top layer consisting of hydrophobic PCL nanofibers, the middle layer containing AgNP-loaded PCL/Gel nanofibers, and the bottom layer composing of hydrophilic PCL/gel nanofiber. Compared with a commercial silver sulfadiazine dressing, the designed wound

dressing showed competitive antimicrobial properties, lower cell toxicity, and accelerated wounds closure for mouse skin injury (161). Hassan et al. (2021) incorporated hydroxyapatite (HAP) doped with different concentrations of silver ions into PCL, and their in vitro cell proliferation assays using human fibroblasts cell lone (HFB4) showed that cells not only grew while in contact with the fibers, but they were also spreading and adhering through the deep pores (162).

In this study, the bacteriophage Fulbright was incorporated into PCL electrospun nanofibers. We examined the stability, cytotoxicity, and antibacterial activity of Fulbright-incorporated nanofiber dressing. This study demonstrates the potential of incorporating Mycobacteriophages into wound dressings as a safe and effective alternative to antibiotics.

## 2. Materials and methods

### 2.1. Media Preparation and Bacterial Strain

*Mycobacterium smegmatis* mc$^2$155 that was provided by the Hatfull lab at the University of Pittsburgh (Pittsburgh, PA, USA) was grown in the standard 7H9 liquid medium complete (7H9 broth base, 0.2% glycerol, albumin dextrose catalase (ADC) (10%V/V), 1 mM calcium chloride ($CaCl_2$)). The liquid cultures were incubated in a shaking incubator (Fisher Scientific # SHKE4450) at 37 °C. On solid media, the bacteria were grown on the standard 7H10 agar plates (0.5% glycerol, 0.2% dextrose, and 1 mM calcium chloride ($CaCl_2$)). The bacteria grown on 7H10 agar plates were incubated at 37 °C. Then, 50 µg/mL of cycloheximide and 50 µg/mL of carbenicillin were added to the liquid culture medium and 7H10 agar plates to reduce contamination. Afterwards, 2X Middlebrook top agar (7H9 broth base, 0.8% agar) was diluted at a 1:1 ratio with 7H9 liquid medium neat (7H9 broth base, 0.2% glycerol, 1 mM calcium chloride ($CaCl_2$) to make 1X Middlebrook top agar, which was used to plate the bacterial lawn. The phage lysate was diluted in phage buffer (pH 7.2, 10 mM Tris, 10 mM magnesium sulfate ($MgSO_4$), 70

mM sodium chloride (NaCl), and 1 mM $CaCl_2$ to quantify the phage. For the agar-overlay method, 10 µL of each dilution was added to 250 µL of *M. smegmatis* $mc^2155$ bacteria and incubated for 10 min. After incubation, 4.5 mL of 1X Middlebrook top agar was added to the bacteria and phage mixture and transferred to a 7H10 agar plate. The plates were incubated at 37 °C and assessed for plaques.

*2.2. Media Preparation and Cell Line*

Balbc/3T3 mouse embryo fibroblast cell line (ATCC #CCL-163) was provided by the Farris lab of Oklahoma Medical Research Foundation (Oklahoma City, OK, USA) and were grown using Dulbecco's Modified Eagle Medium (DMEM) (4500 mg/L glucose, L-glutamine, sodium bicarbonate) (D5796) supplemented with sodium pyruvate (25-000-Cl), and FBS (26140-079). A vial of Balbc/3T3 was thawed and quickly transferred to 10 mL of DMEM supplemented media and centrifuged to remove the dimethyl sulfoxide (DMSO). The supernatant was removed, and the cell pellet was re-suspended in fresh media. The cell solution was transferred to a T25 cell culture flask and incubated at 37 °C, 5%$CO_2$. When 80% confluency was reached, the cells were trypsinized, centrifuged, and re-suspended in fresh media and were split ⅕ every 3–4 days.

*2.3. Polycaprolactone Fiber Production*

PCL and acetone solution mixture were prepared as described in our earlier research (163). Figure 7a,b represents the schematic image of the PCL and PCL_Fulbright nanofiber membrane fabrication processes, respectively. PCL nanofiber membrane was produced by our custom-made electrospinning machine (Figure 8) using the PCL solution and a single axis one-inch discharge metallic needle (aluminum 23 G blunt needle, Model # BX 25). For the PCL_Fulbright membrane, a single-axis needle was replaced by a coaxial metallic needle (100-10-Coaxial-2822, Rame-hard Instrument Co., Succasunna, NJ, USA), which was attached with

two syringe pumps to feed the PCL solution (core) and phage Fulbright suspended in phage buffer solution (shell) into a glass syringe and flowed through a tube to a metallic needle (Figure **8**). The drum collector was spun using speed-controlled direct current (DC) motors. The syringe needle is electrically excited by applying a high voltage (9 kV) produced by a 0–30 kV high-voltage power supply (Model # ES 30, Gamma High Voltage Research Inc., Ormond Beach, FL, USA). This electrically charged syringe needle is positioned above a drum collector to capture the synthetic polymer fiber stream. We have optimized the speed of rotation, the distance between needle and drum, and the deposition rate of fiber on the drum to produce the fiber mat. The distance between the needle and drum collectors was approximately 5 cm. The feeding rate of the core and shell solutions will be adjusted to a rate of 0.025 mL/minute. The nanofiber was deposited on the drum with a 40 mm radius.
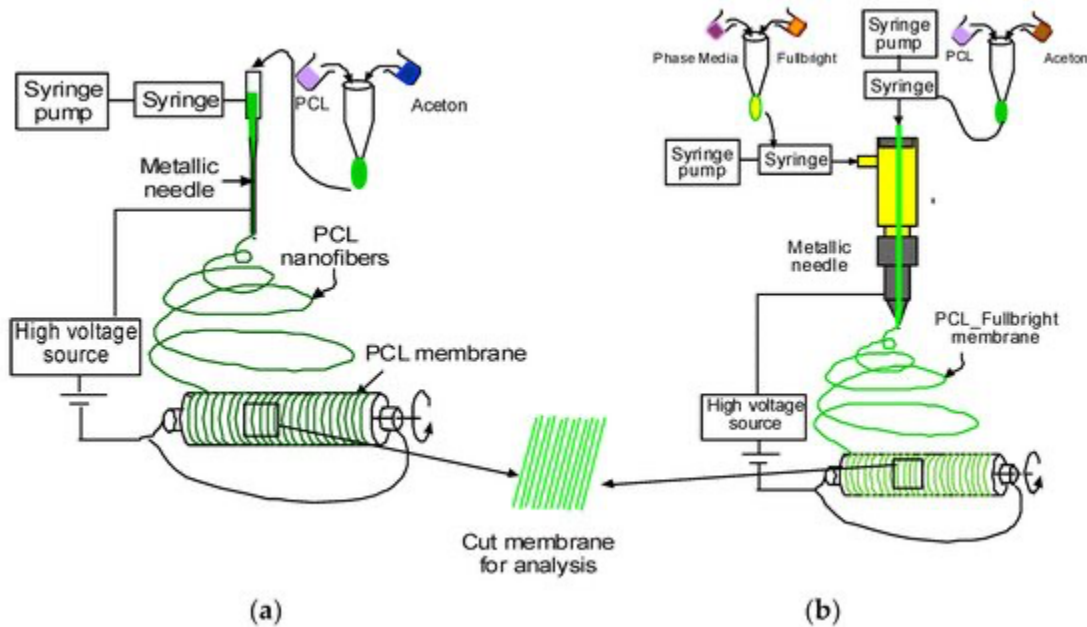
Figure 7. Schematic representation of the production of PCL and PCL_Fulbright nanofiber.

Figure 8. Electrospun fabrication unit used to produce the nanofiber dressing.

*2.4. PEG Purification of Fulbright*

For the preparation of our PCL_Fulbright nanofiber, polyethylene glycol (PEG 8000) purified phage lysate was used. The high titer phage lysate was centrifuged using a Thermo Scientific Sorvall Legend XTR centrifuge at $5500\times g$ at 4 °C for 10 min. The supernatant was transferred to a new tube, and 1 M of NaCl and 10% of PEG were added. The solution was gently stirred at 15 rpm using a VWR Orbital Shaker at 4 °C overnight until the PEG and NaCl were in solution. The sample was then centrifuged at $5500\times g$ at 4 °C for 10 min, and the supernatant was decanted,

ensuring that most of the PEG has been removed. The pellet was gently re-suspended in fresh phage buffer and stirred overnight at 4 °C. Another centrifugation was performed, and the final cell pellet was re-suspended in phage buffer and stored at 4 °C until use. The phage titer in the PEG-purified lysate was $1 \times 10^{13}$ PFU/mL. This lysate was used for all subsequent experiments unless otherwise noted.

## 2.5. Phage Stability and Storage Temperature

We examined the short-term and long-term effects of polycaprolactone on the stability of phage particles. For short-term effect, $\approx 2$ cm$^2$ of control PCL nanofiber was placed in a 5 mL phage lysate, and the tube was incubated at 37 °C. The control for this experiment was phage lysate without PCL fiber stored at 37 °C. The phage titer of the lysate soaked with control PCL was determined using standard agar-overlay methods each day for 7 days. For long-term effect, we tested the infectivity of the control PCL and PCL_Fulbright wound dressing stored at 4 °C and −20 °C at 7 days and 11 months post-production by testing the fiber for clear zones on a host bacterial lawn.

## 2.6. In Vitro Phage Release and Viability Assay

For the phage release assay, we followed the procedure described by Korehei and Kadla (164) with minor modifications. Briefly, $\approx 2$ cm$^2$ of PCL_Fulbright nanofiber was soaked in 3 mL phage lysate for 1 h with gentle shaking using a VWR Orbital Shaker. The soaked fiber was washed in 3 mL of phage buffer, which was shaken at 60 rpm at room temperature. The fibers were transferred into a fresh 3 mL phage buffer solution every 10 min for 10 washes. The PCL fiber was left to air dry for 2 h and stored at 4 °C overnight. The fibers were then plated on the host bacterial lawn and incubated at 37 °C for 48 h. The plates were assessed for clear borders surrounding the phage dressing.

A viability assay was performed to determine the number of phages released from the phage-incorporated fiber. The protocol outlined by Salalha et al. (2006) was followed with few modifications (149). PCL_Fulbright nanofiber cut into $\approx 2$ cm$^2$ segments were placed in a microcentrifuge tube containing 1 mL of phage buffer. The tube was incubated for 60 min at room temperature to allow the phages to release into solution. After incubation, the tube was vortexed, and ten-fold dilutions of the buffer solution were plated using the agar-overlay method. The plates were incubated at 37 °C for 48 h, and PFU/mL was determined.

*2.7. Antimicrobial Assay*

To determine the antimicrobial activity of PCL_Fulbright, we followed the protocol outlined by Noguiera et al. (2017) (5). The bacterial culture was adjusted to $1.5 \times 10^8$ CFU/mL per McFarland standards using a Grant-bio Den-1 McFarland Densitometer. The bacteria were diluted to a final concentration of $1.5 \times 10^6$ CFU/mL, and 1 mL of the bacteria was transferred into each culture tube. PCL and PCL_Fulbright cut into $\approx 2$ cm$^2$ were added to the culture tubes containing bacteria. Another tube containing bacteria alone served as a control. All the tubes were incubated at 37 °C for 24 h. After incubation, the bacterial solution in the culture tubes was diluted using ten-fold dilution and plated on 7H10 agar plates. The plates were incubated at 37 °C for 24 h. To determine the bacterial growth inhibition (% of Inhibition) at 24 h, the following calculation was used:

$$\% \text{ Inhibition} = \frac{C-A}{C} \times 100$$

where *C* is the average value of Colony-Forming Units (CFU) of the controls, and *A* is the average value of CFU of PCL_Fulbright.

## 2.8. Direct Contact Cytotoxicity Assay

Cytotoxicity assays were performed using the protocol outlined by Nogueira (2017) (5) to determine the effect of PCL_Fulbright nanofiber on cell viability. Balbc/3T3 CCL-163 mouse embryo fibroblast cells were grown as recommended by the manufacturer. Cell viability was measured using AlamarBlue (ThermoFisher DAL 1100). Controls for this experiment were wells containing Balbc/3T3 cells alone and wells containing PCL plus cells. This experiment was conducted in quadruplets. For the direct contact assay, 500,000 Balbc/3T3 cells per well were seeded directly on $\approx 2$ cm$^2$ of PCL_Fulbright and PCL. and incubated at 37 °C, 5% CO$_2$ for 24 h. After incubation, AlamarBlue was added as per the manufacturer's recommendation. We transferred 100 µL from each well to a 96-well plate, and the absorbance was measured at 570 nm with a reference wavelength of 600 nm using a Biotek Synergy H1 Hybrid Reader. Random samples from each of the groups were randomly selected for DAPI staining.

## 2.9. DAPI Staining

Fibroblast cells attached to the wound dressing were visualized using fluorescent microscopy. 4′6-Diamidino-2-phenylindole (DAPI) is a commonly used fluorescent dye for staining DNA in cells. Random samples from the cytotoxicity assay were washed three times with phosphate buffer saline (PBS). After the final wash, 4% formalin was used to fix the cells. After fixation, the formalin was aspirated, and the fibers were washed with PBS three times. DAPI staining was performed in the dark at room temperature and was followed by five PBS washes prior to imaging. The morphology of the cell nuclei was observed using Zeiss Axiovert 200 m Inverted Fluorescent Microscope at 20x objective at an excitation wavelength of 350 nm.

## 2.10. Effect of Temperature on Phage Stability

The stability of phage Fulbright was evaluated at different temperatures (20 °C, 30 °C, 40 °C, 45 °C, 50 °C, 55 °C, 60 °C, and 65 °C), following the protocol described in our previous work (106). A 1 mL volume of the phage lysate ($1 \times 10^{12}$ PFU/mL) was dispensed onto a 1.5 mL tube. The tubes were incubated at the above temperatures for 1 h. The temperature-subjected lysates were serially diluted in sterile phage buffer and then plated using the standard agar-overlay method. After 24 h of incubation, the number of PFU/mL was determined and plotted.

## 2.11. Effect of pH on Phage Stability

The stability of the virion particle was determined by incubating the phage in phage buffer adjusted to pH values (3, 4, 5, 6, 7, 8, and 9) for 1 h following the protocol described in our previous publication (106). The pH of the phage buffer was adjusted using HCl or NaOH and was 0.22 μm filter-sterilized. The initial concentration of phage was $1 \times 10^{11}$ PFU/mL, and it was incubated for 1 h at 37 °C. Following the incubation, phage was diluted, plated using the agar-overlay method, and incubated.

## 2.12. Scanning Electron Microscopy

Scanning electron micrographs of PCL and PCL_Fulbright were obtained using the Zeiss Neon 40 EsB. The samples were directly imaged at 50,000× with an accelerating voltage of 5 kV. The interaction between *M. smegmatis* and the PCL_Fulbright nanofiber was imaged using a Thermo Quattro S-Field Emission Environmental Scanning Electron Microscope at 5000× without any staining at an accelerating voltage of 20 kV.

## 2.13. Tensile Strength Assay

This study used a CellScale UniVert biomaterials testing machine (Waterloo, Ontario, Canada) to compare the tensile strength difference between PCL and PCL_Fulbright nanofibers.

Three samples were prepared from a 15 cm × 20 cm piece of PCL and PCL_Fulbright membranes by placing an ASTM D638 standard plastic specimen mold (Figure **9**a) and cutting along the edge of the mold using a razor blade. Figure **9**b,c show the prepared PCL and PCL_Fulbright samples. The dimension of the gauge length section was 10 mm × 3 mm × 0.025 mm (length × width × thickness). Each sample was mounted on the grips (Figure **9**d), and tension tests were conducted using a 100 N load cell with a 1 mm/min rate to each test sample. The load and displacement values were recorded from each experiment until the failure of the samples. The tension modulus and maximum tensile stress were calculated from the calculated stress and strain values from the recorded load and displacement values.



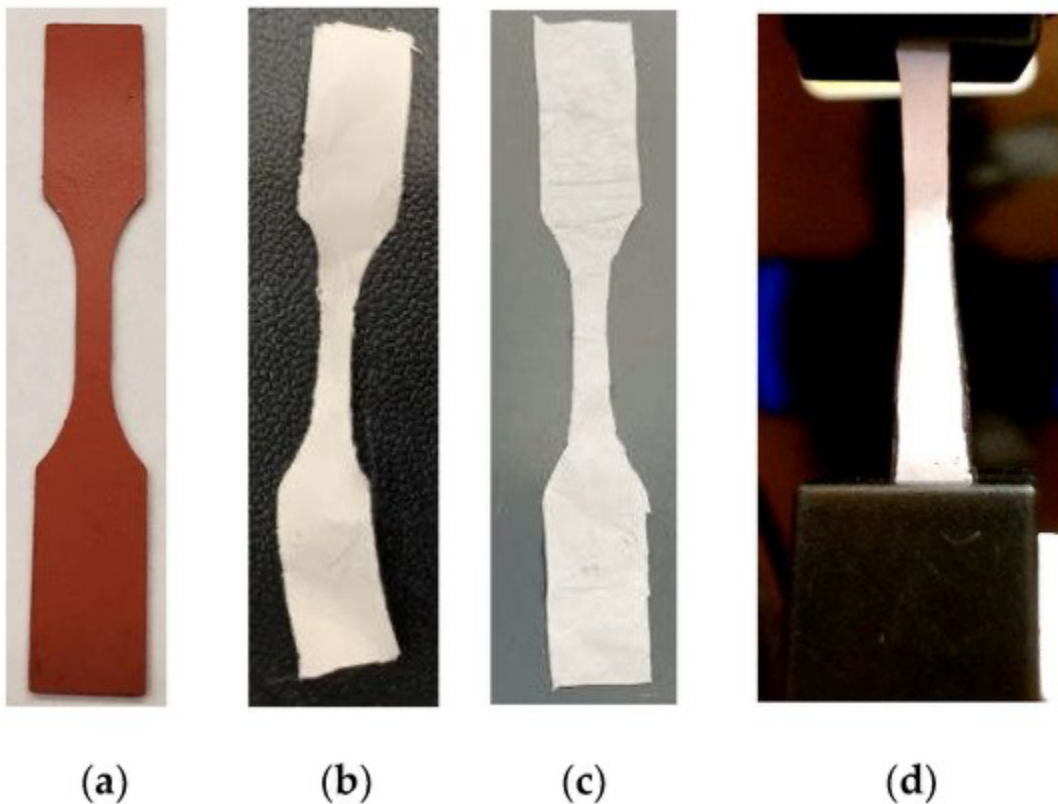(a)            (b)            (c)            (d)

Figure 9. Tensile strength assay. (a) ASTM D638 standard plastic specimen mold used to make tension test specimen. Prepared samples: (b) PCL and (c) PCL_Fulbright. (d) A sample in the gripper during the mechanical tests.

*2.14. Water Absorption Test*

Water absorption tests were conducted of according to a standard method described in detail in our earlier reference (165). Three pieces of PCL and PCL_Fulbright membrane were cut from a fabricated mat, and we soaked each membrane in distilled water for 5 min. Each piece was air-dried for 30 min. Each sample weight before soaking ($W_0$) and after air-dried ($W_t$) was measured using a precision scale. The percentage of water absorption of each sample was measured using ($W_t - W_0$) × 100%/$W_0$ and compared.

*2.15. Statistical Analysis*

Graphpad prism was used to calculate one-way ANOVA and Tukey post hoc tests to establish multiple comparisons between samples. *p*-values below 0.05 were considered statistically significant. All experiments were conducted in triplicate and repeated 3 times unless stated otherwise.

3. Results

*3.1. Phage Stability and Storage Temperature*

The short-term and long-term stability of the phage particle in the PCL_Fulbright nanofiber was examined in our experiments. The stability of Fulbright lysate in the presence of PCL was observed over the course of 7 days at 37 °C. We found no significant difference in phage titer between PCL fiber immersed in the phage lysate and the control phage lysate at 37 °C. *p* values were *p* = 0.9760 (37 °C vs. 37 °C with PCL) (Figure 10E). Our results (Figure 10A–D) indicate that the phage particle loses its infectivity when stored at 4 °C for 7 days, as indicated by the absence of a clear zone (Figure 10B). However, the wound dressings stored at −20 °C retain their antimicrobial activity at day 7 post-production (Figure 10C). There is still some antimicrobial

activity against the host bacteria when stored at −20 °C, even after 11 months indicated by clearing (Figure 10D).
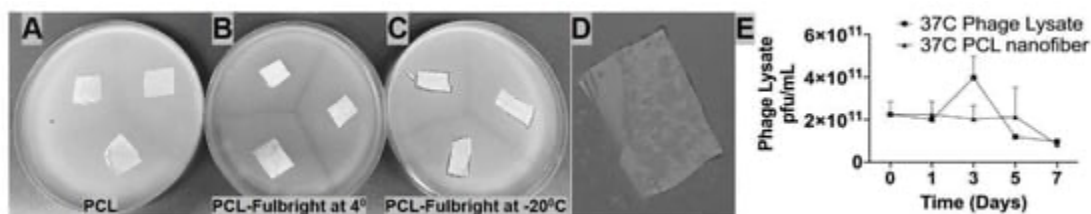


Figure 10.(A-D) Stability of PCL_Fulbright. Panels A–D represent nanofibers stored at different temperatures and time periods. (**A**) PCL nanofiber at 4 °C stored for 7 days, (**B**) PCL_Fulbright at 4 °C for 7 days, (**C**) PCL_Fulbright at −20 °C stored for 7 days (**D**) PCL_Fulbright at −20 °C stored for 11 months. (**E**) Stability of phage particle with PCL nanofiber. All nanofibers were plated on *M. smegmatis* lawn. Arrows are pointing to a clear zone formed by phage lysis of host bacteria.

### 3.2. In Vitro Phage Release and Viability Assay

We examined the release of phage Fulbright from PCL_Fulbright electrospun fibers by submerging the PCL_Fulbright fiber in the phage buffer. We spot tested each of the 10-fold dilutions from each wash. Our results (Figure 11a) show that most of the phage is released in the first 2 h, as indicated by the presence of plaques on plates A through J and a lack of plaques on plate K. However, even with the overnight storage at 4 °C, the phage was still active and lysed the host bacteria. In the phage viability assay, the number of viable phages released per ≈2 cm² of PCL_Fulbright fiber was quantified (Figure 11b). Our results indicate that soaking PCL_Fulbright nanofiber dressing in the phage buffer for 60 min resulted in the release of +/−$2.1 \times 10^5$ PFU/mL infectious particles from the fiber quantified using the standard agar-overlay method.
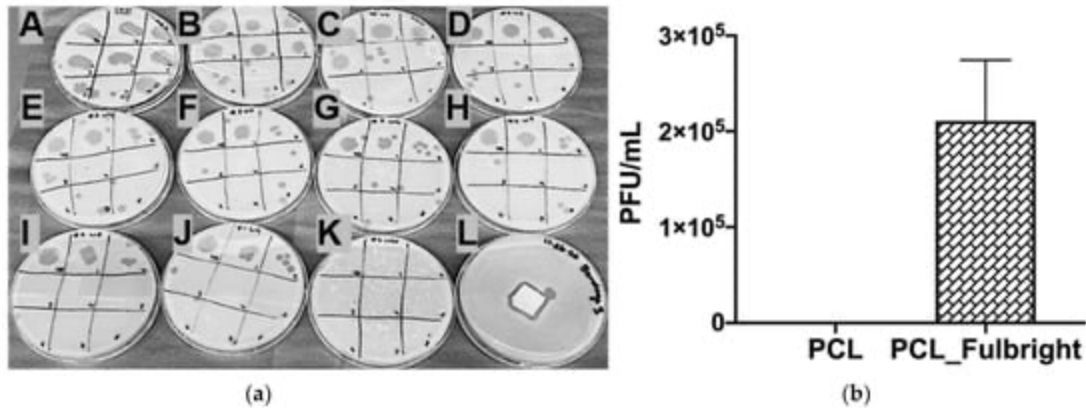
Figure 11 . (a) In vitro phage release and (b) phage viability assay. (a) Each (A–K) represents the spot test of phage buffer after each wash. The spots on each plate represent the 10-fold dilutions of the phage buffer. (A–J) indicate the release of phage Fulbright from the nanofiber into the phage buffer. (K) indicates no residual phages in the phage buffer. (L) shows a clear zone around the washed nanofiber incubated on a lawn of host cells. (b) The graph panel represents the number of viable phage particles in the viability assay.

### 3.3. Antimicrobial Assay

The antimicrobial activity of PCL_Fulbright against *M. smegmatis* was measured at 4 h and 24 h of incubation with $1.5 \times 10^6$ CFU/mL of the host bacteria. At 4 h of incubation, PCL_Fulbright was ineffective at decreasing *M. smegmatis* concentration (data not shown). However, after 24 h, there was a significant difference in bacterial concentration between bacterial control suspension without PCL fiber and PCL_Fulbright (Figure **12**). The *p* values comparing the control and PCL_Fulbright were $p = 0.0049$. The percentage of inhibition was 62.93%.
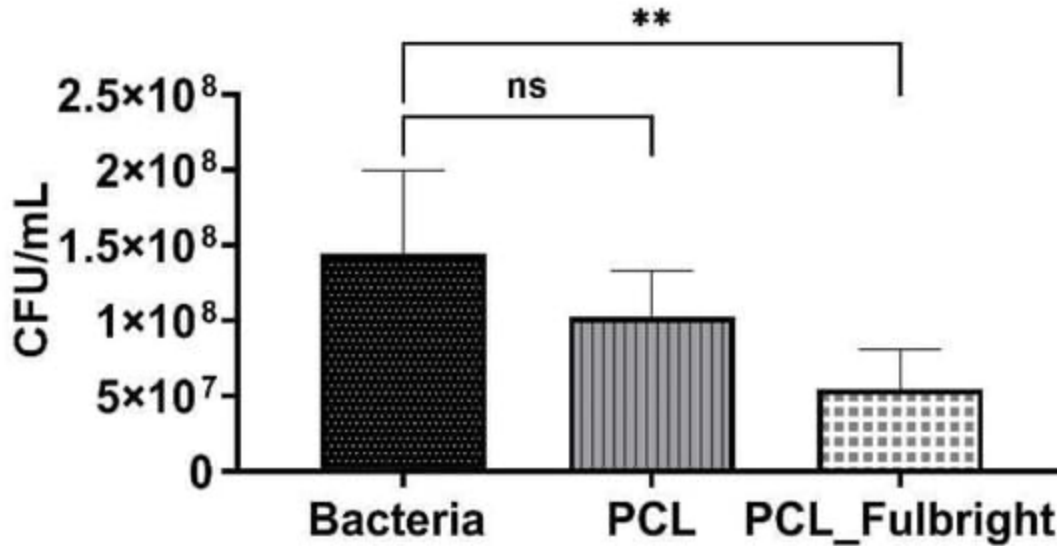
Figure 12. Antimicrobial activity of PCL_Fulbright against *M. smegmatis* at 24 h. ns = no significant difference and ** p value < 0.05

*3.4. Cytotoxicity Assays*

Our cytotoxicity assay did not show any cytotoxic effect of PCL or PCL_Fulbright on the mouse 3T3 fibroblast cell line (Figure **13**). The assay showed average values that did not range beyond 30% from controls. Per Noguiera (2017); only an alteration under or over 30% in comparison with controls would be considered cytotoxic or pro-tumorigenic, respectively (5). The fluorescent microscopy image (Figure **14**) of the cells attached to the PCL and PCL_Fulbright show nuclei with normal phenotype, further supporting that the phage particles in the PCL_Fulbright do not contribute to the cytotoxicity.
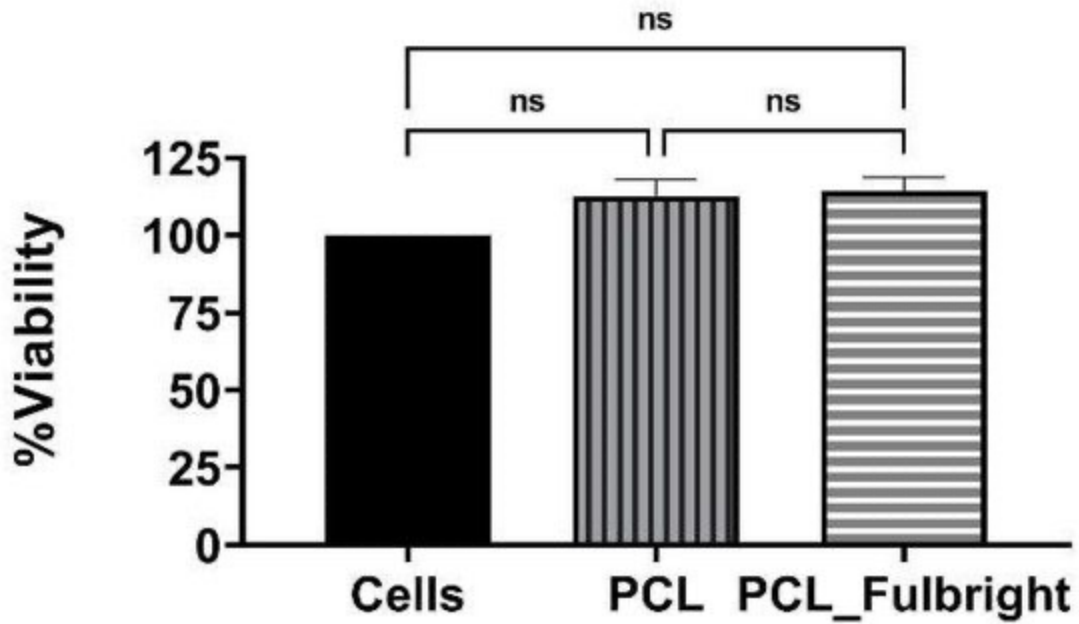
Figure 13. Cytotoxicity assay against Balbc/3T3 mouse embryo fibroblast cell line. ns = no significant difference.
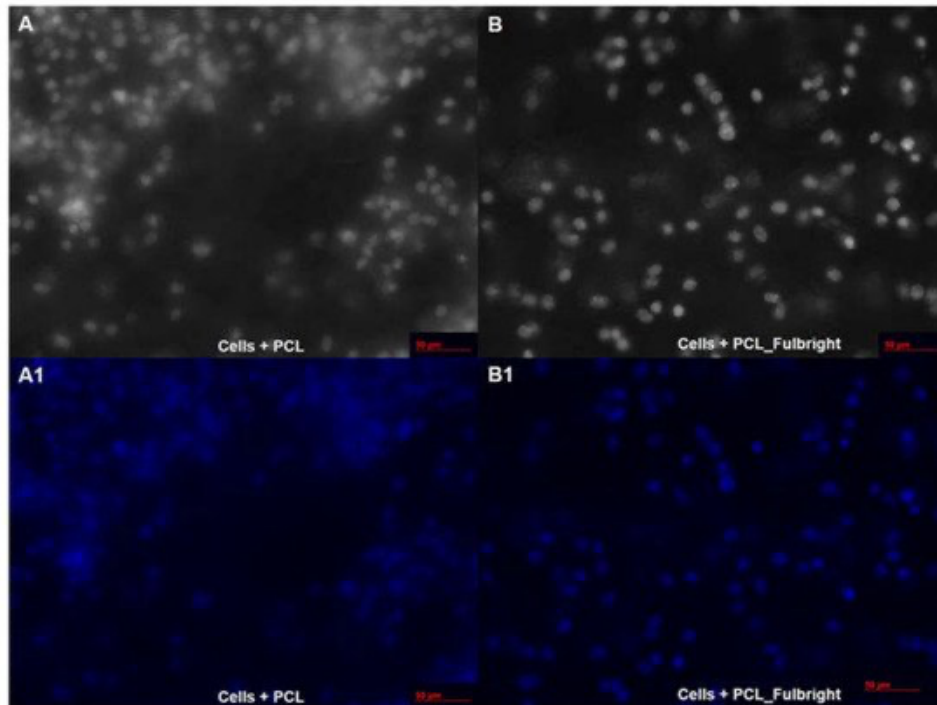


Figure 14. Fluorescent microscopy image of PCL dressing with mouse fibroblasts on top of the wound dressing in black and white (**A**) with DAPI filter (**A1**). (**B,B1**) represent cells on top of the phage incorporated PCL_Fulbright wound dressing.

## 3.5. Thermal and pH Stability of Fulbright

There was no significant change in the infectivity of the phage between 20 and 55 °C. However, there was a 0.2 log reduction at 60 °C and a 4.3 log reduction in infectivity after 1 h at 65 °C (Figure **15**A). At pH 3, there is a 5.69 log reduction in infectivity and with no significant change in the infectivity between 4 and 9 pH (Figure **15**B).
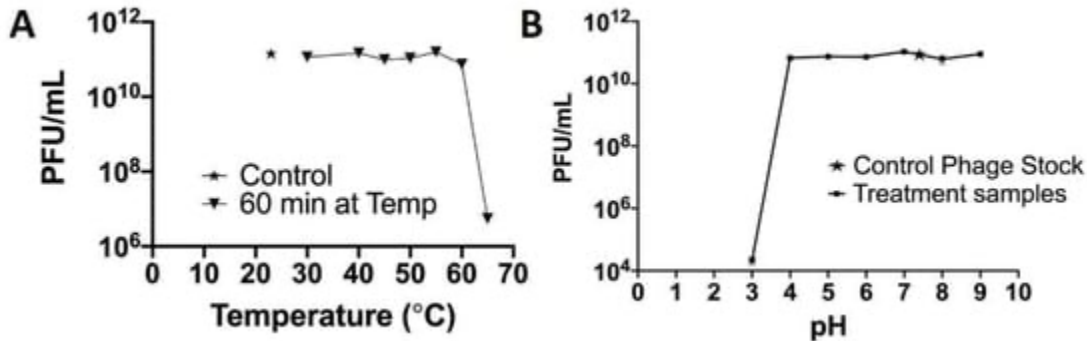


Figure 15. Temperature and pH stability of phage Fulbright.

## 3.6. SEM Imaging

The average diameter of our nanofiber is $\approx 200 \pm 96$ nm. At 50,000× magnification, we can clearly see the incorporated phage particle in the PCL_Fulbright fiber represented by bright spherical spots (Figure 1**6**B,C) as indicated by the arrows. We do not see those spots in the PCL fiber without phage (Figure 1**6**A). We can see the random distribution of phage particles in the nanofiber core. The interaction between the PCL_Fulbright and the bacterial can be clearly seen in Figure 1**7**. The phage particle was uniformly distributed along the length of the fiber. The distribution of phage particle on the fiber was measured from a SEM image. We estimated five phage particles per 500 nm along the fiber distance.
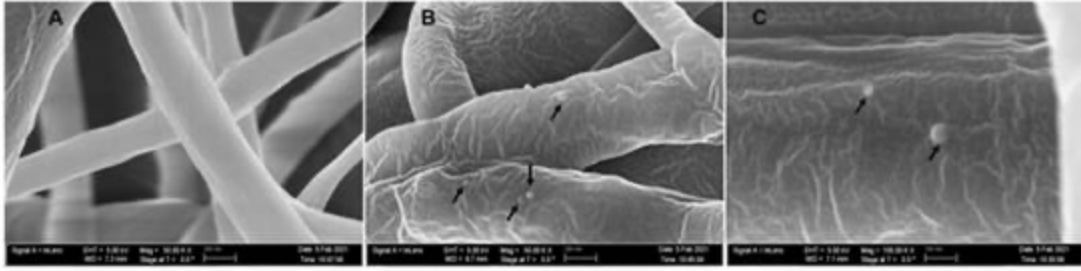
Figure 16. SEM imaging of PCL and PCL_Fulbright. (A) represents PCL nanofiber. (B) is PCL_Fulbright with black arrows pointing to the phage particles. (C) is magnified at 100,000×.
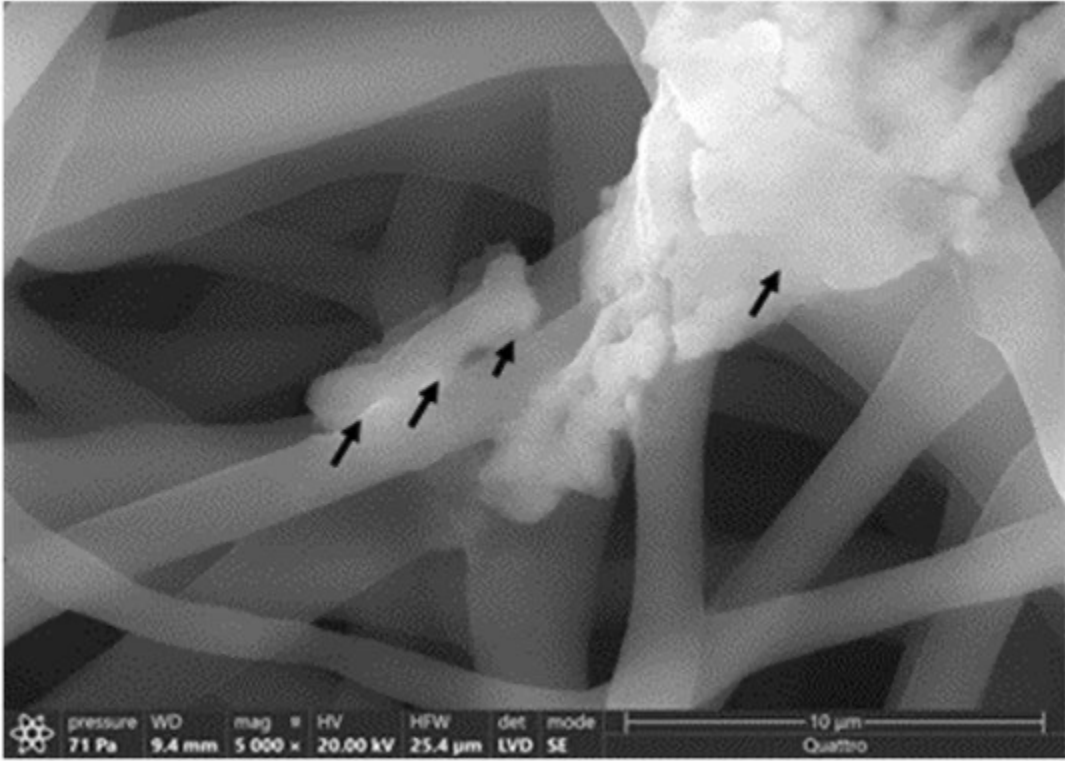


Figure 17. Interaction between *M. smegmatis* and PCL_Fulbright nanofiber. Black arrows are pointing to the bacterial cell attached to the nanofiber.

*3.7. Mechanical Tests*

A clear difference of stress vs. strain curves (Figure 18) and mechanical properties (tensile modulus and strength) calculated from the stress vs. strain results (Table 1) between PCL and PCL_Fulbright samples was observed. Immobilization of Fulbright reduced the tensile strength and modulus significantly ($p$ value < 0.05).



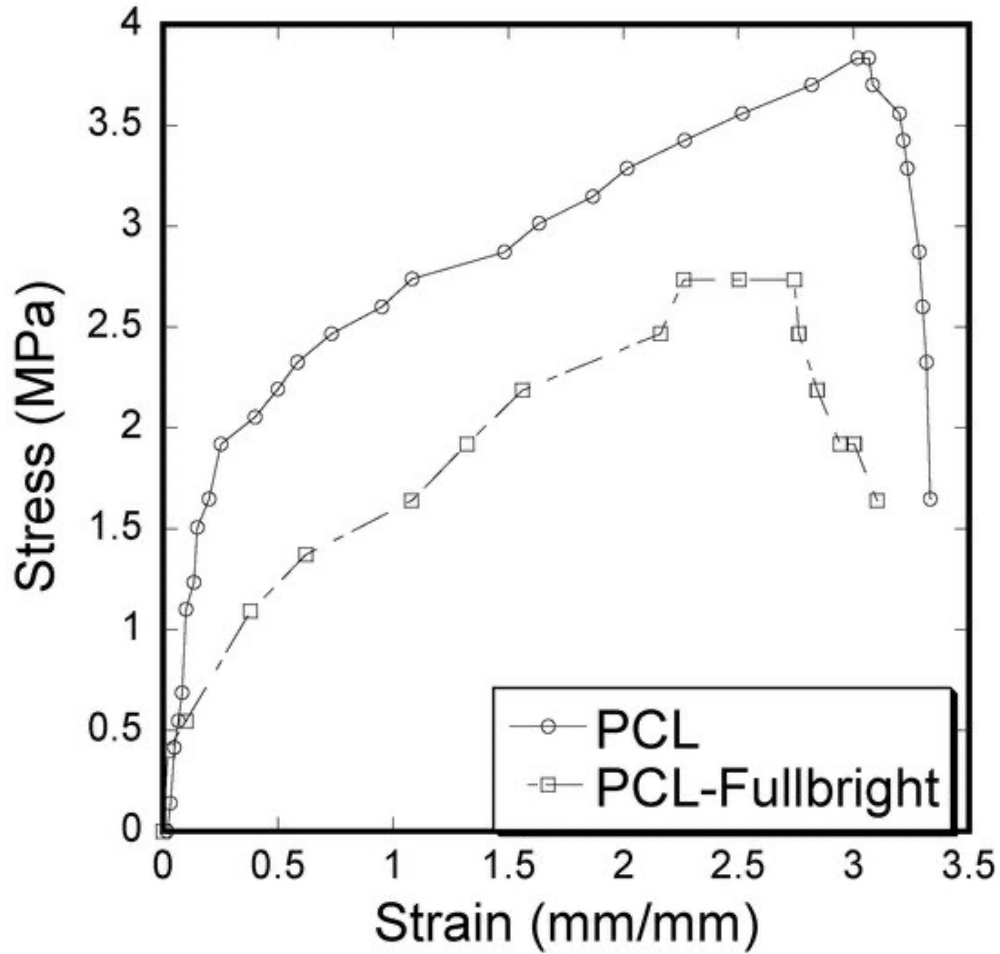Figure 18. Stress–strain curve of pull-out tension tests showing the difference between the strain and stress for PCL and PCL_Fulbright cloths.

Table 1. Mechanical test results of PCL and PCL_Fulbright samples. The data are presented as mean ± standard of error for sample size, n = 3.

| Sample Number | Tensile Strength | | Tensile Modulus | |
|---|---|---|---|---|
| | PCL | PCL_Fulbright | PCL | PCL_Fulbright |

| | | | | |
|---|---|---|---|---|
| 1 | 5.37 | 2.45 | 9.22 | 3.74 |
| 2 | 5.47 | 3.28 | 13.67 | 5.48 |
| 3 | 5.01 | 2.73 | 9.58 | 1.89 |
| | | | | |
| Average | 5.28 | 2.82 | 10.82 | 3.70 |
| St dev | 0.11 | 0.20 | 1.17 | 0.85 |
| *p* value | | 0.00 | | 0.02 |

*3.8. Water Absorption Tests*

A significantly lower amount of water absorption was observed in the PCL membranes compared to the PCL_Fulbright membranes (Figure 1**9**). In our previous study using two different thickness of PCL cloths, we found a negligible water absorption on both PCL cloths. The results mean that phage Fulbright attachment with the PCL fiber makes PCL fiber more hydrophilic.
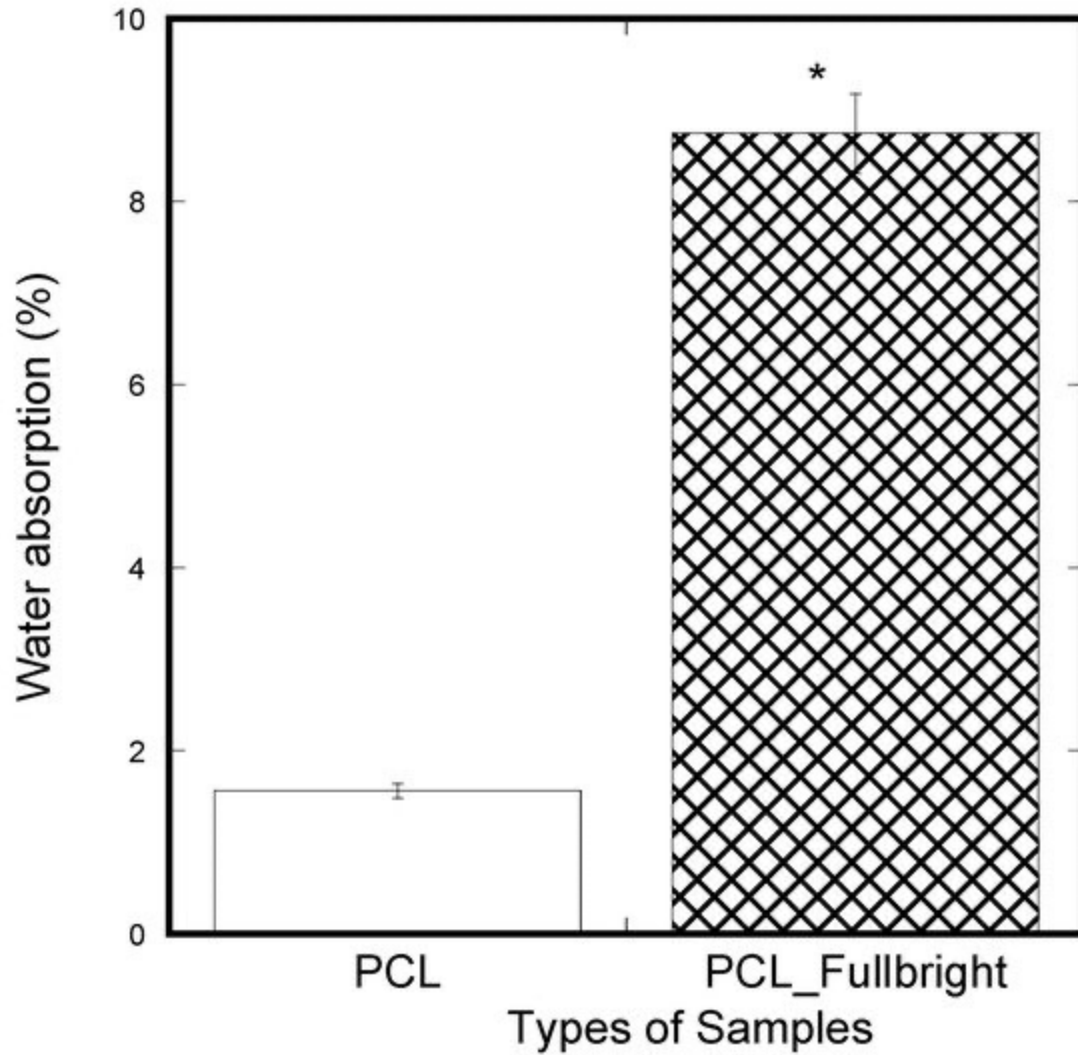
Figure 19. Water absorption of PCL and PCL_Fulbright. Weight percentage difference between the samples from the initial weight after applying soaking in water for 5 min and air-dried for 30 min. The values of all parameters were reported as mean ± SOE (n = 3). * refers $p < 0.05$ with respect to PCL.

**4. Discussion -** Bacteriophages are highly specific and only infect and kill their host bacteria. This quality makes them ideal for treating antibiotic-resistant bacterial skin infections, as they can leave the normal microbiota and human tissues intact. We incorporated a Mycobacteriophage Fulbright into polycaprolactone (PCL) nanofiber dressing, evaluated its stability in the nanofiber matrix, phage release from the nanofiber, its antimicrobial effect on host bacteria, and its cytotoxicity against a mouse fibroblast cell line, Balbc/3T3.

We have evaluated the stability of phage Fulbright in two ways. First, we examined the stability of the particle in contact with PCL, and second, we also assessed its stability when incorporated into the PCL nanofiber. Our results show that there is no significant change in the phage titer when it is in contact with PCL fiber (Figure **10**E) for up to 7 days. When the phage is incorporated into the PCL nanofiber, the ideal storage temperature to retain the phage viability is −20 °C, as we lost the activity after a week when stored at 4 °C. We were able to detect phage activity at −20 °C for up to 11 months. Our results agree with published studies by Nogueira (2017) in terms of PCL being an excellent medium for phage delivery (5). Studies conducted by Koo (2016) further support the effect of storage temperatures on the infectivity of bacteriophages in electrospun nanofibers with higher phage activity at −20 °C (148). These observations are also confirmed by Salhala (2016) and Korehei (2014) (149, 164).

In 2014, Korehei and Kadla (2014) investigated the effects of electrospinning bacteriophage T4 in poly (ethylene oxide) and cellulose diacetate fibers (164). A rapid release of T4 was observed once suspended in an aqueous buffer medium. A release of 100% T4 phage occurred within 30 min of immersion due to the high hydrophilicity of PEO. Our in vitro phage release assay demonstrates that when soaked in phage buffer for about 2 h, an average of $2.11 \times 10^5$ PFU/mL of Fulbright was released per 2 cm$^2$ of nanofiber. However, the wound dressing retained its

antimicrobial activity indicated by a clear zone on a lawn of host bacteria (Figure **11**a, Plate L). The ability of the wound dressing to maintain a slow and sustained release such as ours may be an ideal trait for treating infections caused by slow-growing bacteria.

The antimicrobial activity of PCL_Fulbright wound dressing in contact with *M. smegmatis* culture at 4 h of contact showed no reduction in bacterial concentration. This may be due to the hydrophobic characteristic of PCL fiber and mycolic acid in the *M. smegmatis* cell wall. Previous studies by Yang and Deng demonstrated a reduced adhesion capacity of PCL to bacteria (166). However, at 24 h, there is a percentage inhibition of 62.93%, indicating that once the phages are released into the media, the phages lysed the host cells successfully. We tested the cytotoxic effect of PCL_Fulbright on a mouse fibroblast cell line. Our results indicate that PCL_Fulbright does not have any cytotoxic effect on cells. The direct contact assay showed an average growth enhancement of 14.39% in the presence of phage-incorporated wound dressing. Our previous studies using fibroblasts, osteoblasts, and mesenchymal stem cells with PCL nanofiber also support this observation (167, 169).

As phage Fulbright is subjected to temperature fluctuations during the production of PCL_Fulbright nanofiber, we also examined the infectivity of the phage particles at various temperatures and pHs (Figure **15**). The phage particle is infective up to 60 °C, and there is a 4.3-log reduction at 65 °C. For pH, it appears that highly acidic pH (≤3) disrupts the structure of phage particle. Previous studies have shown that the inability of the phage to form plaques at higher temperatures, highly acidic, and highly basic environments is due to the denaturation of phage and host proteins (169). These data are consistent with our previous work with other Mycobacteriophages in terms of their stability (106, 130, 170, 171).

The stress vs. strain behavior due to tensile force (**Figure 18**) of PCL_Fulbright fibrous membranes was compared with that of pure PCL membrane. As shown in Table 1, PCL fibrous membranes exhibit the higher tensile strength and modulus compared to the values of PCL_Fulbright. The tensile strength values of PCL ($5.28 \pm 0.11$ MPa) were in agreement with the PCL membranes strength found by Cheng et al. The decrease in mechanical properties due to the incorporation of bacteriophages in PCL can be justified with the fact that the wt % of PCL in PCL_Fulbright is less compared to the PCL. The study by Cheng (2018) found that the increase in PCL concentration in PCL with bacteriophages increased the tensile strength (172).

Since water absorption ability is an important parameter for cell adhesion, water absorption tests were performed on the nanofibrous mats. The water absorption of PCL_Fulbright fibrous membranes was compared with that of pure PCL membrane. The result indicated that PCL_Fulbright nanofibers have higher water uptake than PCL nanofibrous mats. The water uptake of PCL_Fulbright compared to PCL nanofiber structures is due to the hydrophilicity of phage Fulbright and morphological differences between the two samples. The higher water absorption of the PCL_Fulbright membrane observed compared to PCL agrees with previous research (173, 174) where it is reported that the presence of protein and porosity might be mainly responsible for the difference between total water uptake values of PCL fiber mats.

Presently, there are commercial antimicrobial applications that have limitations, such as Dermasilk®, which is a silk-based material with Silane quaternary ammonium compounds (Si-QAC). Padycare® and TheraBond® take advantage of Silver's antimicrobial properties. Unfortunately, Si-QAC has been reported to cause bacterial resistance and skin sensitization (5). Although silver has been heavily used as antimicrobial dressings in managing the wound infections of patients, there is a lack of knowledge regarding it effects on the normal healing process of the

body (175). Silver can be toxic to fibroblasts and keratinocytes at high concentrations (176). Nesporova (2020) concluded that silver dressings should only be used in highly infected wounds, as sub-toxic levels of silver could induce intracellular ROS production and DNA breaks, affecting rapidly proliferating cells during the wound-healing process (146).

The limitation of this study is that we did not conduct contact an analysis to measure the sample groups' hydrophobicity. Our previous study on contact angle measurement tests on the various thickness of PCL membranes found that PCL membranes are very hydrophobic (contact angle values varied between 120 and 150 degrees) (163). The contact angle generally shows a linear relation to the absorbed water drop volume, independent of the substrate water absorption rate, drop volume, and contact time (177). This means that a linear decrease in the measured contact angle can be observed with increasing water absorbed drop volume. We have observed a 5.6 times rise in water absorption value due to the incorporation of phage Fulbright with PCL; therefore, a decrease in the contact angle value of Fulbright_PCL is anticipated. Considering a linear relationship between water contact angle and absorbed drop volume, we expect that Fulbright_PCL is still regarded as hydrophobic, since the water contact angle above 90 degrees is considered hydrophobic. Our future study will confirm the hydrophobicity of the Fulbright_PCL sample.

**5. Conclusions -** This study aims to incorporate Mycobacteriophage Fulbright into a polycaprolactone (PCL) nanofiber and test its antimicrobial effect against the host bacteria. We successfully combined PCL's biocompatibility and enhanced the nanofiber's antimicrobial properties against mycobacterial infections by incorporating mycobacteriophages. Our produced phase_PCL nanofiber membranes have the potential for phage therapy trials to treat skin, bloodstream, urinary tract, and other soft tissues infections.

**Institutional Review Board Statement -** Not applicable.

**Informed Consent Statement -** Not applicable.

**Data Availability Statement -** Not applicable.

**Conflicts of Interest -** The authors declare no conflict of interest.

# CHAPTER 5: FUTURE DIRECTIONS

The future direction of this work is filled with many possibilities. First, the electrospinning method could be improved by increasing the porosity of the nanofibers. By decreasing the width of the fiber and production time, there could be more phages loaded in less fiber, increasing the chance of phage release and contact with host bacteria. Second, this phage incorporated wound dressing could be tested on animal models. Diabetic patients are typically at risk for suffering wound infections on their feet that requires treatment that the phage wound dressing can provide. Because of this, the phage wound dressing could be tested on diabetic mice. To do this, the skin of the mice is shaved and punctured to form the wound. Then, the bacteria is inoculated into the wound. After the infection has developed, the phage wound dressing is administered and the wound healing observed.

Third, because superinfection immunity can occur, it is important that the phage nanofiber is effective from the point of contact. Therefore incorporating a cocktail of phages that infect one host could be more effective. A cocktail of phages that infect different strains of bacteria could also prove useful, because wounds are typically infected by multiple strains of bacteria. Lastly, since polycaprolactone is biodegradable, another approach could involve hydrogels. To do this, the PCL dressing layer could be placed on a wound. The bacteriophage is incorporated into the hydrogel and placed on top of the fiber. The bacteriophage can then pass through the nanofiber and into the infected wound. This allows the PCL nanofiber to remain and degrade onto the wound, while the phage incorporated hydrogel can be replaced, minimizing dressing changes and trauma to the wound site.

In conclusion, the incorporation of bacteriophages in wound dressings can be explored in a plethora of ways. However, there are some current limitations that we are facing today. Though

there are several bacteriophages being isolated each day, very few of these phages can infect human pathogens of interest. Thus, huge efforts must be placed on isolating stable bacteriophages. Buffers of differing qualities used to store bacteriophages should also be explored to improve the incorporation of the phage with the fiber.

**CHAPTER 6: CONCLUSIONS**

Multi-drug resistant bacteria are a growing concern in society and have led to researchers seeking alternative treatments. Phage therapy is a promising alternative due to its low cost, specificity, and effectiveness. In this work, we explored phage therapy in two ways. First, we successfully characterized the mycobacteriophage Fulbright and determined that it is a suitable candidate to use for phage therapy due to its stability at a broad range of pH and temperatures. In the context of Fulbright's life cycle with its host, *M. smegmatis,* a latent period of 90 min and rise period of 90 min was observed, with a plateau at 3 hours. Host range assays showed that Fulbright has a wide host range, with the capability of infecting *M. abscessus* at high titer concentrations. Second, phage incorporated PCL nanofiber was characterized and its efficacy was tested against host bacteria. Polycaprolactone was chosen as the vehicle for phage delivery due to its elasticity and biodegradability. After successfully incorporating Fulbright in PCL, PCL_Fulbright was able to infect *M. smegmatis.* PCL_Fulbright remained stable when stored at -20°C for up to 11 months. Lastly, PCL_Fulbright had no cytotoxic or tumorigenic effects against a mouse fibroblast cell line.

In conclusion, this study aimed to highlight the importance of using accepted and suitable methods for phage characterization and lay the foundation for future phage therapy research. This project outlined qualities a phage should possess to be used for therapy: stability under a wide range of environmental conditions and a short (~30-90 min) latent period. Moreover, a phage incorporated wound dressing should demonstrate efficacy against host bacteria, non-cytotoxic, non-tumorigenic, and be easily stored at temperature conditions similar to a standard freezer (-18°C to -20°C). PCL_Fulbright has the potential for phage therapy to treat skin, urinary tract, and other soft tissue infections without causing side effects to the patient. While this model dressing

can still be improved, this project has established methods to properly characterize phage incorporated wound dressings and assess their effectiveness.

# CHAPTER 7: BIBLIOGRAPHY

1.  Vig K, Chaudhari A, Tripathi S, Dixit S, Sahu R, Pillai S, Dennis V, Singh S. (2017). Advances in Skin Regeneration Using Tissue Engineering. Int. J. Mol. Sci.18(4), 789; https://doi.org/10.3390/ijms18040789
2.  Tavakoli S, Klar A. (2020). Advanced Hydrogels as Wound Dressings. Biomolecules.10, 1169; doi:10.3390/biom10081169
3.  Yun S.H., Sim E.H., Park J.I., Han J.Y. (2016). Platelet Activation: The Mechanisms and Potential Biomarkers. Biomed Res. Int.
4.  Lucas T, Waisman A, Ranjan R, Roes J, Krieg T, Muller W, Roers A, Eming S. (2010). Differential Roles of Macrophagegs in Diverse Phases of Skin Repair. J Immunol April 1, 2010, 184(7) 3964-3977; doi: https://doi.org/10.4049/jimmunol.0903356
5.  Nogueira, F., Karumidze, N., Kusradze, I., Goderdzishvili, M., Teixeira, P., & Gouveia, I. C. (2017). Immobilization of bacteriophage in wound-dressing nanostructure. *Nanomedicine*, *13*(8), 2475-2484. https://doi.org/10.1016/j.nano.2017.08.008
6.  Dhivya, S., Padma, V. V., & Santhini, E. (2015). Wound dressings - a review. *BioMedicine*, *5*(4), 22. https://doi.org/10.7603/s40681-015-0022-9
7.  Schreml S, Szeimies RM, Prantl L, Karrer S, Landthaler M, Babilas P. Oxygen in acute and chronic wound healing. Br J Dermatol. (2010). 163(2):257-68. doi: 10.1111/j.1365-2133.2010.09804.x. Epub 2010 Apr 15. PMID: 20394633.
8.  Rajendran, S., & Anand, S.C. (2011). Hi-tech textiles for interactive wound therapies. Handbook of Medical Textiles. Doi: 10.1533/9780857093691.1.38
9.  Lazarus, G. S., Cooper, D. M., Knighton, D. R., Margolis, D. J., Pecoraro, R. E., Rodeheaver, G., & Robson, M. C. (1994). Definitions and guidelines for assessment of wounds and evaluation of healing. *Archives of dermatology*, *130*(4), 489–493.
10. Guo, S., & Dipietro, L. A. (2010). Factors affecting wound healing. *Journal of dental research*, *89*(3), 219–229. https://doi.org/10.1177/0022034509359125
11. Daunton C, Kothari S, Smith L, Steele D. A history of materials and practices for wound management. (2012). Wound Pract Res. 20:174-86.
12. Shah J. B. (2011). The history of wound care. *The journal of the American College of Certified Wound Specialists*, *3*(3), 65–66. https://doi.org/10.1016/j.jcws.2012.04.002
13. Dickson, E.E. (1926) *Surgical Dressing* United States of America, New Brunswick, New Jersey US1612267A. Johnson & Johnson. https://patentimages.storage.googleapis.com/86/b3/4d/874f5df0442006/US1612267.pdf.
14. Sarabahi S. (2012). Recent advances in topical wound care. *Indian journal of plastic surgery : official publication of the Association of Plastic Surgeons of India*, *45*(2), 379–387. https://doi.org/10.4103/0970-0358.101321
15. Ramshaw, J. A., Werkmeister, J. A., & Glattauer, V. (1996). Collagen-based biomaterials. *Biotechnology & genetic engineering reviews*, *13*, 335–382. https://doi.org/10.1080/02648725.1996.10647934
16. Doillon, C. J., & Silver, F. H. (1986). Collagen-based wound dressing: effects of hyaluronic acid and fibronectin on wound healing. *Biomaterials*, *7*(1), 3–8. https://doi.org/10.1016/0142-9612(86)90080-3
17. Ishihara, M., Nakanishi, K., Ono, K., Sato, M., Kikuchi, M., Saito, Y., Yura, H., Matsui, T., Hattori, H., Uenoyama, M., & Kurita, A. (2002). Photocrosslinkable chitosan as a dressing for

wound occlusion and accelerator in healing process. *Biomaterials*, *23*(3), 833–840. https://doi.org/10.1016/s0142-9612(01)00189-2

18. Moshakis, V., Fordyce, M. J., Griffiths, J. D., & McKinna, J. A. (1984). Tegadern versus gauze dressing in breast surgery. *The British journal of clinical practice*, *38*(4), 149–152.

19. Brumberg, V., Astrelina, T., Malivanova, T., & Samoilov, A. (2021). Modern Wound Dressings: Hydrogel Dressings. *Biomedicines*, *9*(9), 1235. https://doi.org/10.3390/biomedicines9091235

20. Thomas, S., & Loveless, P. (1997). A comparative study of the properties of twelve hydrocolloid dressings. *World Wide Wounds*, *1*, 1-12. http://www.worldwidewounds.com/1997/july/Thomas-Hydronet/hydronet.html

21. Thompson T. (2006). *Foam Composite.* United States of America, West Newbury, MA US7048966B2. Hydrophilix,LLC,West Newbury, MA. https://patentimages.storage.googleapis.com/8d/63/83/fe275a1c37aac0/US7048966.pdf

22. Thomas, A., Harding, K. G., & Moore, K. (2000). Alginates from wound dressings activate human macrophages to secrete tumour necrosis factor-alpha. *Biomaterials*, *21*(17), 1797–1802. https://doi.org/10.1016/s0142-9612(00)00072-7

23. Doss, J., Culbertson, K., Hahn, D., Camacho, J., & Barekzi, N. (2017). A Review of Phage Therapy against Bacterial Pathogens of Aquatic and Terrestrial Organisms. *Viruses*, *9*(3), 50. https://doi.org/https://doi.org/10.3390/v9030050

24. Monk, A. B., Rees, C. D., Barrow, P., Hagens, S., & Harper, D. R. (2010). Bacteriophage applications: where are we now? *Letters in Applied Microbiology*, *51*(4), 363-369. https://doi.org/10.1111/j.1472-765x.2010.02916.x

25. Sulakyelidze, A., & Barrow, P. (2004). Phage therapy in animals and agribusiness. *Bacteriophages*. https://doi.org/10.1201/9780203491751.ch13

26. Leitner, L., Ujmajuridze, A., Chanishvili, N., Goderdzishvili, M., Chkonia, I., Rigvava, S., Chkhotua, A., Changashvili, G., McCallin, S., Schneider, M. P., Liechti, M. D., Mehnert, U., Bachmann, L. M., Sybesma, W., & Kessler, T. M. (2021). Intravesical bacteriophages for treating urinary tract infections in patients undergoing transurethral resection of the prostate: a randomised, placebo-controlled, double-blind clinical trial. *Lancet Infect Dis.*, *21*(3), 427-436. https://doi.org/10.1016/S1473-3099(20)30330-3

27. Gorski, A., Borysowski, J., & Międzybrodzki, R. (2020). Phage Therapy: Towards a Successful Clinical Trial. *antibiotics*, *9*(11), 827. https://doi.org/doi:10.3390/antibiotics9110827

28. Dedrick, R. M., Guerrero-Bustamante, C. A., Garlena, R. A., Russell, D. A., Ford, K., Harris, K., Gilmour, K. C., Soothill, J., Jacobs-Sera, D., Schooley, R. T., Hatfull, G. F., & Spencer, H. (2019). Engineered bacteriophages for treatment of a patient with a disseminated drug-resistant Mycobacterium abscessus. *Nature Medicine*, *25*, 730-733. https://doi.org/https://doi.org/10.1038/s41591-019-0437-z

29. Woodings, C. (2003). Fibers, regenerated cellulose. *Kirk-Othmer Encyclopedia of Chemical Technology*. https://doi.org/doi:10.1002/0471238961.1805070523151504.a01.pub2

30. Nemati, S., Kim, S.-j., Shin, Y. M., & Shin, H. (2019). Current progress in application of polymeric nanofibers to tissue engineering. *Nano Convergence*, *6*(36). https://doi.org/https://doi.org/10.1186/s40580-019-0209-y

31. Xue, J., Xie, J., Liu, W., & Xia, Y. (2017). Electrospun Nanofibers: New Concepts, Materials, and Applications. *Accounts of Chemical Research* *50*(8), 1976-1987. https://doi.org/https://doi.org/10.1021/acs.accounts.7b00218

32. Sun, B., Long, Y. Z., Zhang, H. D., Li, M. M., Duvail, J. L., Jiang, X. Y., & Yin, H. L. (2014). Advances in three-dimensional nanofibrous macrostructures via electrospinning. *Progress in Polymer Science*, *39*(5), 862-890. https://doi.org/doi:10.1016/j.progpolymsci.2013.06.002

33. Yang, G. Z., Li, H. P., Yang, J. H., Wan, J., & Yu, D. G. (2017). Influence of Working Temperature on The Formation of Electrospun Polymer Nanofibers. *Nanoscale research letters*, *12*(1), 55. https://doi.org/10.1186/s11671-016-1824-8

34. Cai, E. Z., Teo, E. Y., Jing, L., Koh, Y. P., Qian, T. S., Wen, F., Lee, J. W., Hing, E. C., Yap, Y. L., Lee, H., Lee, C. N., Teoh, S. H., Lim, J., & Lim, T. C. (2014). Bio-conjugated polycaprolactone membranes: a novel wound dressing. *Archives of plastic surgery*, *41*(6), 638–646. https://doi.org/10.5999/aps.2014.41.6.638

35. Carson, D., Jiang, Y., & Woodrow, K. A. (2016). Tunable Release of Multiclass Anti-HIV Drugs that are Water-Soluble and Loaded at High Drug Content in Polyester Blended Electrospun Fibers. *Pharmaceutical research*, *33*(1), 125–136. https://doi.org/10.1007/s11095-015-1769-0

36. Shin, D., Kim, M. S., Yang, C. E., Lee, W. J., Roh, T. S., & Baek, W. (2019). Radially patterned polycaprolactone nanofibers as an active wound dressing agent. *Archives of plastic surgery*, *46*(5), 399–404. https://doi.org/10.5999/aps.2019.00626

37. Opálková Šišková, A., Bučková, M., Kroneková, Z., Kleinová, A., Nagy, Š., Rydz, J., Opálek, A., Sláviková, M., & Eckstein Andicsová, A. (2021). The Drug-Loaded Electrospun Poly(ε-Caprolactone) Mats for Therapeutic Application. *Nanomaterials (Basel, Switzerland)*, *11*(4), 922. https://doi.org/10.3390/nano11040922

38. Eskandarinia, A., Kefayat, A., Agheb, M. *et al.* (2020). A Novel Bilayer Wound Dressing Composed of a Dense Polyurethane/Propolis Membrane and a Biodegradable Polycaprolactone/Gelatin Nanofibrous Scaffold. *Sci Rep* 10, 3063. https://doi.org/10.1038/s41598-020-59931-2

39. Doostmohammadi, M., Forootanfar, H., Shakibaie, M., Torkzadeh-Mahani, M., Rahimi, H.-R., Jafari, E., Ameri, A., & Ameri, A. (2021). Polycaprolactone/gelatin electrospun nanofibres containing biologically produced tellurium nanoparticles as a potential wound dressing scaffold: Physicochemical, mechanical, and biological characterisation. *IET Nanobiotechnology*, *15*(3), 277-290. https://doi.org/https://doi.org/10.1049/nbt2.12020

40. Oviedo, M., Montoya, Y., Agudelo, W., García-García, A., & Bustamante, J. (2021). Effect of Molecular Weight and Nanoarchitecture of Chitosan and Polycaprolactone Electrospun Membranes on Physicochemical and Hemocompatible Properties for Possible Wound Dressing. *Polymers*, *13*(24), 4320. https://doi.org/10.3390/polym13244320

41. Huang, Y., Dan, N., Dan, W., & Zhao, W. (2019). Reinforcement of Polycaprolactone/Chitosan with Nanoclay and Controlled Release of Curcumin for Wound Dressing. *ACS omega*, *4*(27), 22292–22301. https://doi.org/10.1021/acsomega.9b02217

42. Safdari, F., Gholipour, M. D., Ghadami, A., Saeed, M., & Zandi, M. (2022). Multi-antibacterial agent-based electrospun polycaprolactone for active wound dressing. *Progress in biomaterials*, *11*(1), 27–41. https://doi.org/10.1007/s40204-021-00176-1

43. Do Pham, D. D., Jenčová, V., Kaňuchová, M., Bayram, J., Grossová, I., Šuca, H., Urban, L., Havlíčková, K., Novotný, V., Mikeš, P., Mojr, V., Asatiani, N., Košťáková, E. K., Maixnerová, M., Vlková, A., Vítovská, D., Šanderová, H., Nemec, A., Krásný, L., Zajíček, R., … Gál, P. (2021). Novel lipophosphonoxin-loaded polycaprolactone electrospun nanofiber dressing reduces Staphylococcus aureus induced wound infection in mice. *Scientific reports*, *11*(1), 17688. https://doi.org/10.1038/s41598-021-96980-7

44. Domingues, J. M., Teixeira, M. O., Teixeira, M. A., Freitas, D., Silva, S., Tohidi, S. D., Fernandes, R., Padrão, J., Zille, A., Silva, C., Antunes, J. C., & Felgueiras, H. P. (2022). Inhibition of *Escherichia* Virus MS2, Surrogate of SARS-CoV-2, via Essential Oils-Loaded Electrospun Fibrous Mats: Increasing the Multifunctionality of Antivirus Protection Masks. *Pharmaceutics*, *14*(2), 303. https://doi.org/10.3390/pharmaceutics14020303

45. Liao, I. C., Chen, S., Liu, J. B., & Leong, K. W. (2009). Sustained viral gene delivery through core-shell fibers. *Journal of controlled release : official journal of the Controlled Release Society*, *139*(1), 48–55. https://doi.org/10.1016/j.jconrel.2009.06.007

46. Ratner, B. D. (2012). *Biomaterials science: an introduction to materials in medicine* (2 ed.). Elselvier Academic Press.

47. Ulery, B. D., Nair, L. S., & Laurencin, C. T. (2011). Biomedical applications of biodegradable polymers. *Journal of Polymer Science*, *49*(12), 832-864. https://doi.org/https://doi.org/10.1002/polb.22259

48. Gødsbøl K., Christensen, J. J., Karlsmark, T., Jørgensen, B., Klein, B. M., & Krogfelt, K. A. (2006). Multiple bacterial species reside in chronic wounds: a longitudinal study. *Int Wound J*(3), 225-231. https://doi.org/10.1111/j.1742-481X.2006.00159.x

49. Stevens, D. (2006). *Infections of the skin, muscle and soft tissues* (D. Kasper, E. Braunwald, A. Fauci, & e. al., Eds. 16 ed.). McGraw-Hill.

50. Choi, I., Yoo, D. S., Chang, Y., Kim, S. Y., & Han, J. (2021). Polycaprolactone film functionalized with bacteriophage T4 promotes antibacterial activity of food packaging toward Escherichia coli. *Food Chemistry*, *346*. https://doi.org/https://doi.org/10.1016/j.foodchem.2020.128883

51. Lee, S., & Belcher, A. M. (2004). Virus-Based fabrication of micro- and Nanofibers Using Electrospinning. *Nano Letters*, *4*(3), 387-390. https://doi.org/10.1021/nl034911t

52. Donohue, M. J. (2018). Increasing nontuberculous mycobacteria reporting rates and species diversity identified in clinical laboratory reports. *BMC Infectious Diseases*, *18*(163). https://doi.org/https://doi.org/10.1186/s12879-018-3043-7

53. Franco-Paredes, C., Marcos, L. A., Henao-Martínez, A. s. F., Rodríguez-Morales, A. J., Villamil-Gómez, W. E., Gotuzzo, E., & Bonifazh, A. (2019). Cutaneous Mycobacterial Infections. *Clinical Microbiology Reviews*, *32*(1), e00069-00018. https://doi.org/https://doi.org/10 .1128/CMR.00069-18.

54. Holt, J. G., Krieg, N. R., Sneath, P. H. A., Staley, J. T., & Williams, S. T. (2000). *Bergey's Manual of Determinative Bacteriology* (9 ed.). Lippincott Williams and Wilkins.

55. Singh, P., & Cole, S. T. (2011). *Mycobacterium leprae:* genes, pseudogenes, and genetic diversity. *Future Microbiology*, *6*, 57-71. https://doi.org/https://doi.org/10.2217/fmb.10.153.

56. Röltgen, K., Stinear, T. P., & Pluschke, G. (2012). The genome, evolution and diversity of Mycobacterium ulcerans. *Infection, Genetics, and Evolution*, *12*(3), 522-529. https://doi.org/https://doi.org/10.1016/j.meegid.2012.01.018

57. Prasanna, A. N., & Mehra, S. (2013). Comparative Phylogenomics of Pathogenic and Non-Pathogenic Mycobacterium. *PLos One*, *8*(8), e71248. https://doi.org/https://doi.org/10.1371/journal.pone.0071248

58. Bottai, D., Stinear, T. P., Supply, P., & Brosch, R. (2014). Mycobacterial Pathogenomics and Evolution. *Microbiology Spectrum*, *2*(1). https://doi.org/https://doi.org/10.1128/microbiolspec.MGM2-0025-2013xs

59. Stinear, T. P., Seemann, T., Pidot, S., Frigui, W., Reysset, G., Garnier, T., Meurice, G., Simon, D., Bouchier, C., Ma, L., Tichit, M., Porter, J. L., Ryan, J., Johnson, P. D. R., Davies, J. K.,

Jenkin, G. A., Small, P. L. C., Jones, L. M., Tekaia, F., . . . Cole, S. T. (2007). Reductive evolution and niche adaptation inferred from the genome of Mycobacterium ulcerans, the causative agent of Buruli ulcer. *Genome Research*, *17*, 192-200. https://doi.org/https://doi.org/10.1101/gr.5942807.

60. Falkinham III, J. O. (2009). Surrounded by mycobacteria: nontuberculous mycobacteria in the human environment. *Journal of Applied Microbiology*, *107*(2), 356-367. https://doi.org/https://doi.org/10.1111/j.1365-2672.2009.04161.x

61. Adjemian, J., Olivier, K. N., Seitz, A. E., Holland, S. M., & Prevots, D. R. (2012). Prevalence of Nontuberculous Mycobacterial Lung Disease in U.S. Medicare Beneficiaries. *American Journal of Respiratory and Critical Care Medicine*, *185*, 881-886. https://doi.org/https://doi.org/10.1164/rccm.201111-2016OC.

62. Wu, U.-I., Holland, S. M., & (2015). Host susceptibility to non-tuberculous mycobacterial infections. *The Lancet Infectious Diseases*, *15*(8), 968-980. https://doi.org/https://doi.org/10.1016/S1473-3099(15)00089-4

63. Szymanski, E. P., Leung, J. M., Fowler, C. J., Haney, C., Hsu, A. P., Chen, F., Duggal, P., Oler, A. J., McCormack, R., Podack, E., Drummond, R. A., Lionakis, M. S., Browne, S. K., Prevots, D. R., Knowles, M., Cutting, G., Liu, X., Devine, S. E., Fraser, C. M., . . . Holland, S. M. (2015). Pulmonary Nontuberculous Mycobacterial Infection. A Multisystem, Multigenic Disease. *American Journal of Respiratory and Critical Care Medicine*, *195*(5), 618-628. https://doi.org/ https://doi.org/10.1164/rccm.201502-0387OC.

64. Ryu, Y. J., Koh, W.-J., & Daley, C. L. (2016). Diagnosis and Treatment of Nontuberculous Mycobacterial Lung Disease: Clinicians' Perspectives. *Tuberculosis and Respiratory Diseases*, *79*(2), 74-84. https://doi.org/https://doi.org/10.4046/trd.2016.79.2.74

65. Wang, S.-H., & Pancholi, P. (2014). Mycobacterial Skin and Soft Tissue Infection. *Curr Infect Dis Rep*, *16*(438). https://doi.org/https://doi.org/10.1007/s11908-014-0438-5.

66. Mostowy, S., & Behr, M. A. (2005). The Origin and Evolution of Mycobacterium tuberculosis. *Clinics in Chest Medicine*, *26*(2), 207-216. https://doi.org/https://doi.org/10.1016/j.ccm.2005.02.004

67. Behr, M. A. (2008). Mycobacterium du jour: what's on tomorrow's menu? *Microbes and Infection*, *10*(9), 968-972. https://doi.org/https://doi.org/10.1016/j.micinf.2008.07.001

68. Davey, T. F., & Rees, R. J. (1974). The nasal dicharge in leprosy: clinical and bacteriological aspects. *Lepr Rev*, *45*, 121-134. https://doi.org/10.5935/0305-7518.19740014

69. Job, C. K., Jayakumar, J., Kearney, M., & Gillis, T. P. (2008). Transmission of Leprosy: A Study of Skin and Nasal Secretions of Household Contactsof Leprosy Patients Using PCR. *The American Society of Tropical Medicine and Hygeine*, *78*(3), 518-521. https://doi.org/https://doi.org/10.4269/ajtmh.2008.78.518.

70. Shah, M. K., Sebti, A., Kiehn, T. E., Massarella, S. A., & Sepkowitz, K. A. (2001). Mycobacterium haemophilum in Immunocompromised Patients. *Clinical Infectious Diseases*, *33*(3), 330-337. https://doi.org/https://doi.org/10.1086/321894

71. Smith, S., Taylor, G. D., & Fanning, E. A. (2003). Chronic Cutaneous Mycobacterium haemophilum Infection Acquired from Coral Injury. *Clinical Infectious Diseases*, *37*(1), e100-e101. https://doi.org/https://doi.org/10.1086/377267

72. Lindeboom, J. A., Coppenraet, L. E. S. B. v., Soolingen, D. v., Prins, J. M., & Kuijper, E. J. (2011). Clinical Manifestations, Diagnosis, and Treatment of Mycobacterium haemophilum Infections. *Clinical Microbiology Reviews*, *24*, 701-717. https://doi.org/https://doi.org/10.1128/CMR.00020-11.

73. Delafont, V., Mougari, F., Cambau, E., Joyeux, M., Bouchon, D., Héchard, Y., & Moulin, a. L. (2014). First Evidence of Amoebae–Mycobacteria Association in Drinking Water Network. *48*(20), 11872-11882. https://doi.org/https://doi.org/10.1021/es5036255

74. Wallace, J. R., Mangas, K. M., Porter, J. L., Marcsisin, R., Pidot, S. J., Howden, B., Omansen, T. F., Zeng, W., Axford, J. K., Johnson, P. D. R., & Stinear, T. P. (2017). Mycobacterium ulcerans low infectious dose and mechanical transmission support insect bites and puncturing injuries in the spread of Buruli ulcer. *PLoS Negl Trop Dis. 11*, e0005553. https://doi.org/https://doi.org/10.1371/journal.pntd.0005553.

75. Zhang, M., Feng, M., & He, J.-Q. (2017). Disseminated Mycobacterium kansasii infection with cutaneous lesions in an immunocompetent patient. *Medical Imagery*, *62*, 59-63. https://doi.org/https://doi.org/10.1016/j.ijid.2017.07.006

76. Kim, C.-J., Kim, N.-H., Song, K.-H., Choe, P. G., Kim, E. S., Park, S. W., Kim, H.-B., Kim, N.-J., Kim, E.-C., Park, W. B., & Oh, M.-d. (2013). Differentiating rapid- and slow-growing mycobacteria by difference in time to growth detection in liquid media. *Diagn Microbiol Infect Dis*, *75*(1), 73-76. https://doi.org/10.1016/j.diagmicrobio.2012.09.019

77. Gordon, R., & Smith, M. (1953). RAPIDLY GROWING, ACID FAST BACTERIA I. Species' Descriptions of Mycobacterium phlei Lehmann and Neumann and Mycobacterium smegmatis (Trevisan) Lehmann and Neumann. *Journal of Bacteriology*, *66*(1), 41-48.

78. Beltan, E., Horgen, L., & Rastogi, N. (2000). Secretion of cytokines by human macrophages upon infection by pathogenic and non-pathogenic mycobacteria. *Microb Pathog*, *28*(5), 313-318. https://doi.org/10.1006/mpat.1999.0345.

79. Brooks, G. F., Caroll, K. C., Butel, J. S., Morse, S. A., & Mietzner, T. A. (2010). *Medical Microbiology* (Jawetz, Melnick, & Adelbergs, Eds. 25 ed.). McGraw-Hill Companies.

80. Snapper, S. B., Melton, R. E., Mustafa, S., Kieser, T., & Jr, W. R. J. (1990). Isolation and characterization of efficient plasmid transformation mutants of Mycobacterium smegmatis. *Molecular Microbiology*, *4*(11), 1911-1919.

81. Griffith, D. E., Aksamit, T., Brown-Elliott, B. A., Catanzaro, A., Daley, C., Gordin, F., Holland, S. M., Horsburgh, R., Huitt, G., Iademarco, M. F., Iseman, M., Olivier, K., Ruoss, S., Reyn, C. F. v., Richard J. Wallace, J., & Winthrop, K. (2007). An Official ATS/IDSA Statement: Diagnosis, Treatment, and Prevention of Nontuberculous Mycobacterial Diseases. *American Thoracic Society Documents*, *175*, 367-416. https://doi.org/https://doi.org/10.1164/rccm.200604-571ST.

82. Forbes, B. A., Hall, G. S., Miller, M. B., Novak, S. M., Rowlinson, M.-C., Salfinger, M., Somoskövi, A., Warshauer, D. M., & Wilson, M. L. (2018). Practical Guidance for Clinical Microbiology Laboratories: Mycobacteria. *Clinical Microbiology Reviews*, *2018*(31), e00038-00017. https://doi.org/https://doi.org/10.1128/CMR.00038-17.

83. Aitken, M. L., Limaye, A., Pottinger, P., Whimbey, E., Goss, C. H., & Tonelli, M. R. (2012). Respiratory Outbreak of Mycobacterium abscessus Subspecies massiliense in a Lung Transplant and Cystic Fibrosis Center. *American Journal of Respiratory and Critical Care Medicine*, *185*(2), 231-232. https://doi.org/https://doi.org/10.1164/ajrccm.185.2.231.

84. Bryant, J. M., Grogono, D. M., Greaves, D., Foweraker, J., Roddick, I., & Inns, T. (2013). Whole-genome sequencing to identify transmission of Mycobacterium abscessus between patients with cystic fibrosis: a retrospective cohort study. *The Lancet*, *381*(9877), 1151-1560. https://doi.org/https://doi.org/10.1016/S0140-6736(13)60632-7

85. Johansen, M. D., & Kremer, L. (2020). CFTR Depletion Confers Hypersusceptibility to Mycobacterium fortuitum in a Zebrafish Model. *Front Cell Infect Mirobiol*, *10*(357). https://doi.org/10.3389/fcimb.2020.00357

86. Johansen, M. D., Alcaraz, M., Dedrick, R. M., Roquet-Banères, F., Hamela, C., Hatfull, G. F., & Kremer, L. (2021). Mycobacteriophage–antibiotic therapy promotes enhanced clearance of drug-resistant Mycobacterium abscessus. *Dis Model Mech*, *14*(9). https://doi.org/10.1242/dmm.049159

87. Henkle, E., & Winthrop, K. (2015). Nontuberculous Mycobacteria Infections in Immunosuppressed Hosts. *Clinics in Chest Medicine*, *36*(1), 91-99. https://doi.org/https://doi.org/10.1016/j.ccm.2014.11.002

88. Mougari, F., Guglielmetti, L., Raskine, L., Sermet-Gaudelus, I., Veziris, N., & Cambau, E. (2016). Infections caused by Mycobacterium abscessus: epidemiology, diagnostic tools and treatment. *Expert Review of Anti-infective Therapy*, *14*(12), 1139-1154. https://doi.org/https://doi.org/10.1080/14787210.2016.1238304

89. Marion, E., Song, O.-R., Christophe, T., Babonneau, J., Fenistein, D., Eyer, J., Letournel, F., Henrion, D., Clere, N., Paille, V., Guérineau, N. C., André, J.-P. S., Gersbach, P., Altmann, K.-H., Stinear, T. P., Comoglio, Y., Sandoz, G., Preisser, L., Delneste, Y., . . . Brodin, P. (2014). Mycobacterial Toxin Induces Analgesia in Buruli Ulcer by Targeting the Angiotensin Pathways. *Cell*, *157*, 1565-1576. https://doi.org/https://doi.org/10.1016/j.cell.2014.04.040.

90. Hendrix, R. W. (2003). Bacteriophage genomics. *Current Opinion in Microbiology*, *6*(5), 506-511. https://doi.org/https://doi.org/10.1016/j.mib.2003.09.004

91. Suttle, C. A. (2007). Marine viruses — major players in the global ecosystem. *Nature Reviews Microbiology*, *5*, 801-812. https://doi.org/doi:10.1038/nrmicro1750

92. Hatfull, G. F., & Hendrix, R. W. (2011). Bacteriophages and their genomes. *Current Opinion in Microbiology*, *1*(4), 298-303. https://doi.org/https://doi.org/10.1016/j.coviro.2011.06.009

93. Hendrix, R. W., Smith, M. C. M., Burns, R. N., Ford, M. E., & Hatfull, G. F. (1999). Evolutionary relationships among diverse bacteriophages and prophages: All the world's a phage. *Proceedings of the National Academy of Sciences of the United States of America*, *96*(5), 2192-2197. https://doi.org/ https://www.jstor.org/stable/47036

94. Zlotnick, A., Reddy, V. S., Dasgupta, R., Schneemann, A., Jr., W. J. R., Rueckert, R. R., & Johnson, J. E. (1994). Capsid assembly in a family of animal viruses primes an autoproteolytic maturation that depends on a single aspartic acid residue. *Journal of Biological Chemistry*, *269*(18), 13680-13684. https://doi.org/https://doi.org/10.1016/S0021-9258(17)36883-7

95. Reguera, J., Carreira, A., Riolobos, L., Almendral, J. M. a., & Mateu, M. G. (2004). Role of interfacial amino acid residues in assembly, stability, and conformation of a spherical virus capsid. *PNAS*, *9*, 2724-2729. https://doi.org/www.pnas.org?cgi?doi?10.1073?pnas.0307748101

96. Yoshiyuki, I., Saori, O., Keiko, T., & Tadahito, K. (2005). Human papillomavirus 16 minor capsid protein L2 help capsomeres assemble independently of intercapsomeric disulfide bonding. *Virus Genes*, *31*(3), 321-328.

97. Madigan, M. T., Martinko, J. M., Stahl, D. A., & Clark, D. P. (2012). *Brock Biology of Microorganisms* (13 ed.). Pearson Education Inc.

98. Knipe, D. M., & Howley, P. M. (2001). *Fundamental Virology* (4 ed.). Lippincott Williams & Wilkins.

99. Hatful, G. F. (2012). The Secret Lives of Mycobacteriophages. *Advances in Virus Research*, *82*. https://doi.org/10.1016/B978-0-12-394621-8.00015-7

100. Allué-Guardia, A., Saranathan, R., Chan, J., & Torrelles, J. B. (2021). Mycobacteriophages as Potential Therapeutic Agents against Drug-Resistant Tuberculosis. *Int J Mol Sci*, *22*(735). https://doi.org/10.3390/ijms22020735

101. Goode, D. (1983). Bacteriophage typing of strains of Mycobacterium tuberculosis from Nepal. *Tubercle*, *64*(1), 15-21. https://doi.org/10.1016/0041-3879(83)90045-4.

102. N/A. (2022). *Host Genus: Mycobacterium*. Retrieved June 21, 2022 from phagesdb.org

103. Samaddar, S., Grewal, R. K., Sinha, S., Ghosh, S., Roy, S., & Gupta, S. K. D. (2016). Dynamics of Mycobacteriophage-Mycobacterial Host Interaction: Evidence for Secondary Mechanisms for Host Lethality. *Appl Environ Microbiol*, *82*(1), 124-133. https://doi.org/10.1128/AEM.02700-15

104. Miller, E. S., Kutter, E., Mosig, G., Arisaka, F., Kunisawa, T., & Rüger, W. (2003). Bacteriophage T4 Genome. *Microbiol Mol Biol Rev*, *67*(1), 86-156. https://doi.org/10.1128/MMBR.67.1.86-156.2003

105. Kotturi, H., Lopez-Davis, C., Nijfarjam, S., Kedy, C., Byrne, M., Barot, V., & Khandaker, M. (2022). Incorporation of Mycobacteriophage Fulbright into Polycaprolactone Electrospun Nanofiber Wound Dressing. *Polymers*, *14*(10), 1948. https://doi.org/https://doi.org/10.3390/polym14101948

106. Patton, C., & Kotturi, H. (2019). Investigating the Growth Characteristics and Infectivity of a Newly Isolated Bacteriophage Against Mycobacterium smegmatis mc2 155. . *Proc. Okla. Acad. Sci.* , *99*.

107. Montso, P. K., Mlambo, V., & Ateba, C. N. (2019). Characterization of Lytic Bacteriophages Infecting Multidrug-Resistant Shiga Toxigenic Atypical Escherichia coli O177 Strains Isolated From Cattle Feces. *Front Public Health*, *7*, 355. https://doi.org/https://doi.org/10.3389/fpubh.2019.00355

108. Feng, Y. Y., Ong, S. L., Hu, J. Y., Tan, X. L., & Ng, W. J. (2003). Effects of pH and temperature on the survival of coliphages MS2 and Qb. *J Ind Microbiol Biotechnol*, *30*(549-552). https://doi.org/10.1007/s10295-003-0080-y

109. Shan, J., Korbsrisate, S., Withatanung, P., Adler, N. L., Clokie, M. R. J., & Galyov, E. E. (2014). Temperature dependent bacteriophages of a tropical bacterial pathogen. *Front Microbiol*, *5*, 599. https://doi.org/10.3389/fmicb.2014.00599

110. Groman, N. B., & Suzuki, G. (1962). TEMPERATURE AND LAMBDA PHAGE REPRODUCTION. *J Bacteriol*, *84*(3), 431-437. https://doi.org/10.1128/jb.84.3.431-437.1962

111. Eshima, N., Fukii, S., Murotsu, T., & Horiuchi, T. (1972). Lambda Phage Mutants Insensitive to Temperature-Sensitive Repressor III. Effects of virL, virR or virC mutation on the gene expression. *Molecular and General Genetics MGG*, *116*, 84-87. https://doi.org/https://doi.org/10.1007/BF00334262

112. Lieb, M. (1979). Heat-sensitive lambda repressors retain partial activity during bacteriophage induction. *J Virol*, *32*(1), 162-166. https://doi.org/10.1128/jvi.32.1.162-166.1979

113. Suzuki, M., Matsumoto, S., Mizoguchi, M., Hirata, S., Takagi, K., Hashimoto, I., Yamano, Y., Ito, M., Fleischmann, P., Winterhalter, P., Morita, T., & Watanabe, N. (2002). Identiˆcation of (3S, 9R)- and (3S, 9S)-Megastigma-6,7-dien-3,5,9-triol 9-O-b-D-glucopyranosides as Damascenone Progenitors in the Flowers of Rosa damascena Mill. *Biosci Biotechnol Biochem*, *66*(12), 2692-2697. https://doi.org/https://doi.org/10.1271/bbb.66.2692

114.   McDaniel, L. D., delaRosa, M., & Paul, J. H. (2006). Temperate and lytic cyanophages from the Gulf of Mexico. *Journal of the Marine Biological Association of the United Kingdom*, *86*(3), 517-527. https://doi.org/doi:10.1017/S0025315406013427

115.   Chu, T.-C., Murray, S. R., Hsu, S.-F., Vega, Q., & Lee, L. H. (2012). Temperature-induced activation of freshwater Cyanophage AS-1 prophage. *Acta Histochem*, *113*(3), 294-299. https://doi.org/10.1016/j.acthis.2009.11.003

116.   Cantrell, K. (2019). *Environmental Effects on Mycobacteriophage Cepens* University of North Georgia]. Nighthawks Open Institutional Repository. https://digitalcommons.northgeorgia.edu/honors_theses/46

117.   Yin, Y., Ni, P. e., Liu, D., Yang, S., Almeida, A., Guo, Q., Zhang, Z., Deng, L., & Wang, D. (2019). Bacteriophage potential against Vibrio parahaemolyticus biofilms. *Food Control*, *98*, 156-163. https://doi.org/https://doi.org/10.1016/j.foodcont.2018.11.034

118.   Hu Z, Meng XC, Liu F. Isolation and characterisation of lytic bacteriophages against *Pseudomonas* spp., a novel biological intervention for preventing spoilage of raw milk. *Int Dairy J.* (2016) 55:72–8. doi: 10.1016/j.idairyj.2015.11.011

119.   Stalin N, Srinivasan P. Efficacy of potential phage cocktails against *Vibrio harveyi* and closely related *Vibrio* species isolated from shrimp aquaculture environment in the south east coast of India. *Vet Microbiol.* (2017) 207:83–96. doi: 10.1016/j.vetmic.2017.06.006

120.   Yin, Y., Ni, P. e., Liu, D., Yang, S., Almeida, A., Guo, Q., Zhang, Z., Deng, L., & Wang, D. (2019). Bacteriophage potential against Vibrio parahaemolyticus biofilms. *Food Control*, *98*, 156-163. https://doi.org/https://doi.org/10.1016/j.foodcont.2018.11.034

121.   Baliga, S., Muglikar, S., & Kale, R. (2013). Salivary pH: A diagnostic biomarker. *J Indian Soc Periodontol*, *17*(4), 461-465. https://doi.org/10.4103/0972-124X.118317

122.   Hopkins, E., Sanvictores, T., & Sharma, S. (2022). Physiology, Acid Base Balance. *StatPearls [Internet]*. https://www.ncbi.nlm.nih.gov/books/NBK507807/

123.   Bennison, L., Miller, C., Summers, R., Minnis, A., Sussman, G., & McGuiness, W. (2017). The pH of wounds during healing and infection: a descriptive literature review. *Cambridge Media*, *25*(2), 63-69. https://journals.cambridgemedia.com.au/application/files/7615/8493/4721/Bennison.pdf

124.   Fujimori, S. (2020). Gastric acid level of humans must decrease in the future. *World J Gastroenterol*, *26*(43), 6706-6709. https://doi.org/10.3748/wjg.v26.i43.6706

125.   Kalapala, Y. C., Sharma, P. R., & Agarwal, R. (2020). Antimycobacterial Potential of Mycobacteriophage Under Disease-Mimicking Conditions. *Front Microbiol*, *11*, 583661. https://doi.org/10.3389/fmicb.2020.583661

126.   Bavda, V. R., & Jain, V. (2020). Deciphering the Role of Holin in Mycobacteriophage D29 Physiology. *Front Microbiol*. https://doi.org/https://doi.org/10.3389/fmicb.2020.00883

127.   Fan, X., Yan, J., Xie, L., Zeng, L., III, R. F. Y., & Xie, J. (2016). Genomic and proteomic features of mycobacteriophage SWU1 isolated from China soil. *Gene*, *561*(1), 45-53. https://doi.org/10.1016/j.gene.2015.02.053

128.   Kraiss, J. P., Gelbart, S. M., & Juhasz, S. E. (1973). A Comparison of Three Mycobacteriophages. *Journal of General Virology*, *20*(1). https://www.microbiologyresearch.org/content/journal/jgv/10.1099/0022-1317-20-1-75?crawler=true

129.   Samaddar, S., Grewal, R. K., Sinha, S., Ghosh, S., Roy, S., & Gupta, S. K. D. (2016). Dynamics of Mycobacteriophage-Mycobacterial Host Interaction: Evidence for Secondary

Mechanisms for Host Lethality. *Appl Environ Microbiol*, *82*(1), 124-133. https://doi.org/10.1128/AEM.02700-15

130.    Ali, A. K., & Kotturi, H. (2019). Isolation of Four Mycobacteriophages from Oklahoma Soil and Testing Their Infectivity Against Mycobacterium abscessus. *Proceedings of the Oklahoma Academy of Science*, *98*, 18-23.

131.    Sethiya, J. P., Sowards, M. A., Jackson, M., & North, E. J. (2020). MmpL3 Inhibition: A New Approach to Treat Nontuberculous Mycobacterial Infections. *Int J Mol Sci*, *21*(17), 6202. https://doi.org/10.3390/ijms21176202

132.    Kurosu, M. (2019). *Cell Wall Biosynthesis and Latency During Tuberculosis Infections* (J. Cirillo & Y. Kong, Eds.). Springer Nature Switzerland AG. https://link.springer.com/content/pdf/10.1007/978-3-030-25381-3_1.pdf

133.    Marrakchi, H., Lanéelle, M.-A., & Daffé, M. (2014). Mycolic acids: structures, biosynthesis, and beyond. *Chem Biol*, *21*(1), 67-85. https://doi.org/10.1016/j.chembiol.2013.11.011

134.    Takayama, K., Wang, C., & Besra, G. S. (2005). Pathway to Synthesis and Processing of Mycolic Acids in Mycobacterium tuberculosis. *Clin Microbiol Rec*, *18*(1), 81-101. https://doi.org/10.1128/CMR.18.1.81-101.2005

135.    Chanishvili, N. (2012). Phage therapy--history from Twort and d'Herelle through Soviet experience to current approaches. *Adv Virus Res*, *83*, 3-40.

136.    Lin, D., Koskella, B., & Lin, H. (2017). Phage therapy: An alternative to antibiotics in the age of multi-drug resistance. *World Journal of Gastrointestinal Pharmacology and Therapeutics*, *8*(3), 162-173.

137.    Ackermann, H.-W., & Ackermann, H.-W. (2011). The first phage electron micrographs. *Bacteriophage*, *1*(4), 225-227. https://doi.org/https://doi.org/10.4161/bact.1.4.17280

138.    Carlton, R. M. (1999). Phage Therapy: Past History and Future Prospects. *Archivum Immunologiae et Therapiae Experimentalis*, *47*, 267-274.

139.    Weber-Dabrowska, B., Mylczyk, M., & Górski, A. (2000). Bacteriophage Therapy of Bacterial Infections: an Update of Our Institute's Experience. *Archivum Immunologiae et Therapiae Experimentalis*, *48*, 547-551.

140.    Lee, M.-R., Sheng, W.-H., Hung, C.-C., Yu, C.-J., Lee, L.-N., & Hsueh, P.-R. (2015). Mycobacterium abscessus Complex Infections in Humans. *Emerging Infectious Diseases*, *21*(9), 1638-1646. https://doi.org/http://dx.doi.org/10.3201/eid2109.141634

141.    Nessar, R., Cambau, E., Reyrat, J. M., Murray, A., & Gicquel, B. (2012). Mycobacterium abscessus: a new antibiotic nightmare. *Journal of Antimicrobial Chemotherapy*, *67*, 810-818. https://doi.org/10.1093/jac/dkr578

142.    Prevention, C. f. D. C. a. (2019). Antibiotic Resistance Threats in the United States. *U.S. Centers for Disease Control and Prevention*. https://doi.org/http://dx.doi.org/10.15620/cdc:82532.

143.    Simões, D., Miguel, S., Ribiero, M., Coutinho, P., Mendonca, A., & Correia, I. (2018). Recent advances on antimicrobial wound dressing: A review. *Elselvier*, *127*, 139-141. https://doi.org/https://doi.org/10.1016/j.ejpb.2018.02.022

144.    Burnham, J. P., Kirby, J. P., & Kollef, M. H. (2016). Diagnosis and management of skin and soft tissue infections in the intensive care unit: a review. *Intensive Care Med*, *42*, 1899-1911. https://doi.org/10.1007/s00134-016-4576-0

145. Cardona, A. F., & Wilson, S. E. (2015). Skin and Soft-Tissue Infections: A Critical Review and the Role of Telavancin in Their Treatment. *Clin Infect Dis*, *61*, S69-S78. https://doi.org/10.1093/cid/civ528

146. Nešporová, K., Pavlík, V. c., Šafránková, B., Vágnerová, H., Odráška, P., Žídek, O. e., Císařová, N. l., Skoroplyas, S., Kubala, L. s., & Velebný, V. r. (2020). Effects of wound dressings containing silver on skin and immune cells. *Scientific Reports*, *10*(15216). https://doi.org/https://doi.org/10.1038/s41598-020-72249-3

147. Fish, R., Kutter, E., Wheat, G., Blasdel, B., Kutateladze, M., & Kuhl, S. J. (2016). Bacteriophage treatment of intransigent diabetic toe ulcers: a case series. *Journal of wound care*, *25*(Sup7). https://doi.org/doi:10.12968/jowc.2016.25.7.s27

148. Koo, C. K., Senecal, K., Senecal, A., & Nugen, S. R. (2016). Dehydration of bacteriophages in electrospun nanofibers: Effect of excipients in polymeric solutions. *Nanotechnology*, *27*(48), 485102. https://doi.org/10.1088/0957-4484/27/48/485102

149. Salalha, W., Kuhn, J., Dror, Y., & Zussman, E. (2006). Encapsulation of bacteria and viruses in electrospun nanofibres. *Nanotechnology*, *17*, 4675-4681. https://doi.org/doi:10.1088/0957-4484/17/18/025

150. Reneker, D., & Yarin, A. (2008). Electrospinning jets and polymer nanofibers. *Polymer*, *49*(10), 2387-2425. https://doi.org/https://doi.org/10.1016/j.polymer.2008.02.002

151. Salam, A., Hassan, T., Jabri, T., Riaz, S., Khan, A., Iqbal, K. M., Khan, S. U., Wasim, M., Shah, M. R., Khan, M. Q., & Kim, I. S. (2021). Electrospun Nanofiber-Based Viroblock/ZnO/PAN Hybrid Antiviral Nanocomposite for Personal Protective Applications. *Nanomaterials (Basel, Switzerland)*, *11*(9), 2208. https://doi.org/10.3390/nano11092208

152. Dowlath, S., Campbell, K., Al-Barwani, F., Young, V. L., Young, S. L., Walker, G. F., & Ward, V. K. (2021). Dry Formulation of Virus-Like Particles in Electrospun Nanofibers. *Vaccines*, *9*(3), 213. https://doi.org/10.3390/vaccines9030213

153. Kazsoki, A., Palcsó, B., Alpár, A., Snoeck, R., Andrei, G., & Zelkó, R. (2022). Formulation of acyclovir (core)-dexpanthenol (sheath) nanofibrous patches for the treatment of herpes labialis. *International journal of pharmaceutics*, *611*, 121354. https://doi.org/10.1016/j.ijpharm.2021.121354

154. Rezk, A. I., Kim, K. S., & Kim, C. S. (2020). Poly(ε-Caprolactone)/Poly(Glycerol Sebacate) Composite Nanofibers Incorporating Hydroxyapatite Nanoparticles and Simvastatin for Bone Tissue Regeneration and Drug Delivery Applications. *Polymers*, *12*(11), 2667. https://doi.org/10.3390/polym12112667

155. Bose, S., Sarkar, N., & Banerjee, D. (2018). Effects of PCL, PEG and PLGA polymers on curcumin release from calcium phosphate matrix for *in vitro* and *in vivo* bone regeneration. *Materials today. Chemistry*, *8*, 110–120. https://doi.org/10.1016/j.mtchem.2018.03.005

156. Huang, Y. J., Huang, C. L., Lai, R. Y., Zhuang, C. H., Chiu, W. H., & Lee, K. M. (2021). Microstructure and Biological Properties of Electrospun In Situ Polymerization of Polycaprolactone-Graft-Polyacrylic Acid Nanofibers and Its Composite Nanofiber Dressings. *Polymers*, *13*(23), 4246. https://doi.org/10.3390/polym13234246

157. Ahmed, M.; Ramadan, R.; El-Dek, S.; Uskoković, V. (2019). Complex relationship between alumina and selenium-doped carbonated hydroxyapatite as the ceramic additives to electrospun polycaprolactone scaffolds for tissue engineering applications. J. Alloys Compd. 801, 70–81.

158. Ahmed, M.; Al-Wafi, R.; Mansour, S.; El-Dek, S.; Usković, V. (2020).Physical and biological changes associated with the doping of carbonated hydroxyapatite/polycaprolactone core-shell nanofibers dually, with rubidium and selenite. J. Mater. Res. Technol. 9, 3710–3723.

159. Christen, M. O., & Vercesi, F. (2020). Polycaprolactone: How a Well-Known and Futuristic Polymer Has Become an Innovative Collagen-Stimulator in Esthetics. *Clinical, cosmetic and investigational dermatology*, *13*, 31–48. https://doi.org/10.2147/CCID.S229054

160. Sisson, A.L.; Ekinci, D.; Lendlein, A. (2013). The contemporary role of ε-caprolactone chemistry to create advanced polymer architectures. *Polymers.* 54, 4333–4350.

161. He, C., Liu, X., Zhou, Z., Liu, N., Ning, X., Miao, Y., Long, Y., Wu, T., & Leng, X. (2021). Harnessing biocompatible nanofibers and silver nanoparticles for wound healing: Sandwich wound dressing versus commercial silver sulfadiazine dressing. *Materials science & engineering. C, Materials for biological applications*, *128*, 112342. https://doi.org/10.1016/j.msec.2021.112342

162. Hassan, A. A., Radwan, H. A., Abdelaal, S. A., Al-Radadi, N. S., Ahmed, M. K., Shoueir, K. R., & Hady, M. A. (2021). Polycaprolactone based electrospun matrices loaded with Ag/hydroxyapatite as wound dressings: Morphology, cell adhesion, and antibacterial activity. *International journal of pharmaceutics*, *593*, 120143. https://doi.org/10.1016/j.ijpharm.2020.120143

163. Khandaker, M., Progri, H., Arasu, D. T., Nikfarjam, S., & Shamim, N. (2021). Use of Polycaprolactone Electrospun Nanofiber Mesh in a Face Mask. *Materials*, *15*, 4272. https://doi.org/10.3390/ma14154272

164. Korehei, R., & Kadla, J. (2014). Encapsulation of T4 bacteriophage in electrospun poly(ethylene oxide)/cellulose diacetate fibers. *Carbohydr Polym*, *100*, 150-157. https://doi.org/10.1016/j.carbpol.2013.03.079

165. Khandaker, M., Alkadhem, N., Progri, H., Nikfarjam, S., Jeon, J., Kotturi, H., & Vaughan, M. B. (2022). Glutathione Immobilized Polycaprolactone Nanofiber Mesh as a Dermal Drug Delivery Mechanism for Wound Healing in a Diabetic Patient. *MDPI Processes*, *10*(3), 512. https://doi.org/https://doi.org/10.3390/pr10030512

166. Yang, H., & Deng, Y. (2008). Preparation and physical properties of superhydrophobic papers. *Journal of Colloid and Interface Science*, *325*(2), 588-593. https://doi.org/https://doi.org/10.1016/j.jcis.2008.06.034

167. Khandaker, M., Kotturi, H., Progri, H., Tummala, S., Nikfarjam, S., Rao, P., Hosna, A., Arasu, D. T., Williams, W., & Haleem, A. M. (2021). In vitro and in vivo effect of polycaprolactone nanofiber coating on polyethylene glycol diacrylate scaffolds for intervertebral disc repair. *Biomed Mater*, *16*(4). https://doi.org/10.1088/1748-605X/abfd12

168. Kotturi, H., Abuabed, A., Zafar, H., Sawyer, E., Pallipparambil, B., Jamadagni, H., & Khandaker, M. (2017). Evaluation of Polyethylene Glycol Diacrylate-Polycaprolactone Scaffolds for Tissue Engineering Applications. *J Funct Biomater*, *8*(3), 39. https://doi.org/10.3390/jfb8030039

169. Koster, S., Evilevitch, A., Jeembaeva, M., & Weitz, D. (2009). Influence of Internal Capsid Pressure on Viral Infections by Phage λ. *Biophysical Journal*, *97*(6), 1525-2529. https://doi.org/10.1016/j.bpj.2009.07.007

170. Kotturi, H., Sahi, U., Kedy, C., & Alib, A. K. (2021). Complete Genome Sequence of Mycobacteriophage Fulbright. *Microbiol Resour Announc*, *10*(11). https://doi.org/10.1128/MRA.00123-21

171.    Ali, A. K., & Kotturi, H. (2019). Isolation of Four Mycobacteriophages from Oklahoma Soil and Testing Their Infectivity Against Mycobacterium abscessus. *Proceedings of the Oklahoma Academy of Science*, *98*, 18-23.

172.    Cheng,W., Zhang, Z., Xu, R., Cai, P., Kristensen, P., Chen, M., & Huang, Y. (2018). Incorporation of bacteriophages in polycaprolactone/collagen fibers for antibacterial hemostatic dual-function. *J Biomed Mater Res B Appl Biomater*, *6*(7), 2588-2595. https://doi.org/doi: 10.1002/jbm.b.34075

173.    Renkler, N. Z., Ergene, E., Gokyer, S., Ozturk, M. T., Huri, P. Y., & Tuzlakoglu, K. (2021). Facile modification of polycaprolactone nanofibers with egg white protein. *J Mater Sci Mater Med*, *32*(4), 34. https://doi.org/10.1007/s10856-021-06505-x

174.    Dwivedi, R., Kumar, S., Pandey, R., Mahajan, A., Nandana, D., Katti, D. S., & Mehrotra, D. (2019). Polycaprolactone as biomaterial for bone scaffolds: Review of literature. *J Oral Biol Craniofac Res*, *10*(1), 381-388. https://doi.org/10.1016/j.jobcr.2019.10.003

175.    International Consensus. Appropriate Use of Silver Dressings in Wounds. An Expert Working Group Consensus; Wounds International: London, UK, 2012.

176.    Khansa, I., Schoenbrunner, A. R., Kraft, C. T., & Janis, J. E. (2019). Silver in Wound Care-Friend or Foe?: A Comprehensive Review. *Plast Reconstr Surg Glob Open*, *7*(8), e2390. https://doi.org/10.1097/GOX.0000000000002390

177.    Krainer, S., & Hirn, U. (2021). Contact angle measurement on porous substrates: Effect of liquid absorption and drop size. *Colloids and Surfaces A: Physicochemical and Engineering Aspects*, *619*, 125603. https://doi.org/https://doi.org/10.1016/j.colsurfa.2021.126503